AD NUMBER
AD339915
CLASSIFICATION CHANGES
TO: unclassified
FROM: secret
LIMITATION CHANGES
TO: Approved for public release, distribution unlimited
FROM: Distribution authorized to DoD only; Administrative/Operational Use; MAR 1957. Other requests shall be referred to Defense Atomic Support Agency, Washington, DC.
AUTHORITY
DNA ltr dtd 6 Jun 1980; DNA ltr dtd 6 Jun 1980

AD 339915L

Operation TEAPOT

NEVADA TEST SITE

February – May 1955

Project 8.1

MEASUREMENT OF DIRECT AND GROUND-REFLECTED THERMAL RADIATION AT ALTITUDE

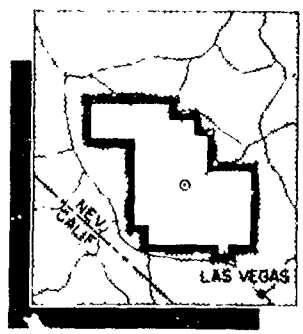

HEADQUARTERS FIELD COMMAND, ARMED FORCES SPECIAL WEAPONS PROJECT
SANDIA BASE, ALBUQUERQUE, NEW MEXICO

Inquiries relative to this report may be made to

Chief, Armed Forces Special Weapons Project
Washington, D. C.

If this report is no longer needed, return to

AEC Technical Information Service Extension
P. O. Box 401
Oak Ridge, Tennessee

AEC Technical Information Service Extension
Oak Ridge, Tennessee

1-4166
41

This document consists of 54 pages,
No. 145 of 210 copies, Series A.

WT-1143

OPERATION TEAPOT—PROJECT 8.1

Report to the Test Director

MEASUREMENT OF DIRECT AND GROUND-REFLECTED THERMAL RADIATION AT ALTITUDE [U]

A. Kviljord

Naval Air Material Center
Philadelphia, Pennsylvania

MARCH 1957

SUMMARY SHOT DATA

SHOT	CODE NAME	DATE	TIME *	AREA	TYPE	LATITUDE & LONGITUDE OF GROUND ZERO
1	Wasp	18 February	1200	T-7-4 1/	762' Air	37° 05' 11.6856" 116° 01' 18.7366"
2	Moth	22 February	0545	T-3	300' Tower	37° 02' 52.2654" 116° 01' 15.6967"
3	Tesla	1 March	0530	T-9b	300' Tower	37° 07' 31.5737" 116° 02' 51.0077"
4	Turk	7 March	0520	T-2	500' Tower	37° 08' 18.4944" 116° 07' 03.1679"
5	Hornet	12 March	0520	T-3a	300' Tower	37° 02' 25.4043" 116° 01' 31.3674"
6	Bee	22 March	0505	T-7-1a	500' Tower	37° 05' 41.3880" 116° 01' 25.5474"
7	ESS	23 March	1230	T-10a	67' Underground	37° 10' 06.1263" 116° 02' 37.7010"
8	Apple	29 March	0455	T-4	500' Tower	37° 05' 43.9200" 116° 06' 09.9040"
9	Wasp'	29 March	1000	T-7-4 2/	740' Air	37° 05' 11.6856" 116° 01' 18.7366"
10	HA	6 April	1000	T-5 3/	36620' MSL Air	37° 01' 43.3642" 116° 03' 28.2624"
11	Post	9 April	0430	T-9c	300' Tower	37° 07' 19.6965" 116° 02' 03.8860"
12	MET	15 April	1115	FF	400' Tower	36° 47' 52.6887" 115° 55' 44.1086"
13	Apple 2	5 May	0510	T-1	500' Tower	36° 03' 11.1095" 116° 06' 09.4937"
14	Zucchini	15 May	0500	T-7-1a	500' Tower	37° 05' 41.3880" 116° 01' 25.5474"

* APPROXIMATE LOCAL TIME - PST PRIOR TO 24 APRIL, PDT AFTER 24 APRIL
1/ ACTUAL GROUND ZERO 36' NORTH, 426' WEST OF T-7-4
2/ ACTUAL GROUND ZERO 94' NORTH, 62' WEST OF T-7-4
3/ ACTUAL GROUND ZERO 36' SOUTH, 397' WEST OF T-5

ABSTRACT

The purpose of this project was to perform measurements of the thermal energy received by aircraft positioned at various distances from nuclear detonations. Measurements were to be made to study the contribution of thermal radiation reflected from the earth's surface to the total radiation received by the aircraft. Ninety-degree-field-of-view calorimeters and radiometers were used to record the thermal radiation under two conditions: (1) calorimeters and radiometers oriented to include radiation received directly from the fireball and (2) calorimeters and radiometers oriented to receive ground-reflected radiation from the earth's surface directly below the test aircraft. Total spectrum and broad-band spectral measurements were made in each case. An ancillary phase of this project was to obtain the temperature rise and decay from thermal radiation in aircraft skin specimens both exposed to and shielded against the effects of aerodynamic cooling.

Recorded total thermal energy data for the two situations above based on 12 aircraft test positions are reported herein, together with an experimental check on existing theoretical treatments. Also reported are thermal energies recorded under broad-band filters and related temperature data of aircraft skin samples exposed to and shielded against the free airstream.

It is concluded that: (1) the theoretical values for the reflected radiation are comparable within 10 percent to the experimental values; the contribution of atmospheric scattered radiation cannot be neglected and in the case where fine particles of matter (like dust) exist in the vicinity of the explosion, the contribution of the scattered radiation increases; (2) random scatter in ground-reflected energy measurements under broad band filters prevent the establishment of a ground-reflected to direct-energy spectral distribution ratio; and (3) aerodynamic cooling had no appreciable effect on the temperature in exposed skin specimens at indicated airspeeds of 175 knots insofar as reducing the maximum temperature rise of 175 degrees Fahrenheit attained by similar specimens shielded from the airstream.

It is recommended that: (1) analytical data for predicting the ratio of ground-reflected to direct radiation be considered valid provided proper allowance is made for atmospheric attenuation and scattering; (2) an experimental check of analytical data be made for weapons exceeding 43-kiloton total yield to further evaluate ground and atmospheric reflection, attenuation, and scattering effects; (3) a further evaluation be made of the effects of surface coating damage to aircraft skin temperatures when thermal field pulse inputs reported herein are utilized in lieu of rectangular pulses.

FOREWORD

This is one of the reports presenting the results of the 56 projects participating in the Military Effects Tests Program of Operation TEAPOT, which included 14 test detonations. For readers interested in other pertinent test information, reference is made to WT-1153, "Summary Report of the Technical Director," Military Effects Program. This summary report includes the following information of possible general interest: (1) an overall description of each detonation, including yield, height of burst, ground zero location, time of detonation, ambient atmospheric conditions at detonation, etc., for the 14 shots; (2) discussion of all project results; (3) a summary of each project, including objectives and results; and (4) a complete listing of all reports covering the Military Effects Tests Program.

PREFACE

The test program reported herein was successfully accomplished through the combined efforts of many individuals, both military and civilian, representing many different agencies. Although individual acknowledgments cannot be made here, the following is a list of the organizations who contributed to the success of this program: Bureau of Aeronautics of the Navy; Directorate of Weapons Effects Tests, Armed Forces Special Weapons Project; Naval Air Special Weapons Facility; Naval Air Missile Test Center; Naval Radiological Defense Laboratory; Douglas Aircraft Company, Inc., El Segundo Division; Naval Ordnance Test Station; Air Force Cambridge Research Center; Wright Air Development Center; and Air Force Special Weapons Center.

CONTENTS

ABSTRACT 3

FOREWORD 4

PREFACE 4

CHAPTER 1 INTRODUCTION 9

1.1 General 9
1.2 Project Objectives 10

CHAPTER 2 EXPERIMENT DESIGN 11

2.1 Background and Theory 11
2.1.1 Thermal Radiation 11
2.1.2 Temperature Rise in Aircraft Skin Panels 14
2.1.3 Spectral Composition of Direct and Reflected Radiation . . . 14
2.2 Test Procedures and Conditions 14
2.3 Instrumentation 17
2.3.1 General Arrangement 17
2.3.2 Instrumentation Equipment 17

CHAPTER 3 RESULTS 18

3.1 Calorimeter Data 18
3.2 Radiometer Data 18
3.3 Skin Sample Temperature Data 18

CHAPTER 4 DISCUSSION 23

4.1 Experimental Check on Analytical Data 23
4.1.1 General 23
4.1.2 Data Reduction Procedure 23
4.1.3 Correlation of Data 37
4.2 Recorded Thermal Data 37
4.3 Spectral Energy Distribution 37
4.4 Temperature Data 38

CHAPTER 5 CONCLUSIONS AND RECOMMENDATIONS 50

5.1 Conclusions 50
5.1.1 Experimental Check on Analytical Data 50
5.1.2 Spectral Energy Distribution 50
5.1.3 Temperature Data 50
5.1.4 Operational Success 50
5.2 Recommendations 50

5.2.1 Thermal Data 50
5.2.2 Temperature Data 50

APPENDIX 51

REFERENCES 52

FIGURES

2.1 Ratio of Reflected to Direct Radiation 12
2.2 Ratio of Reflected to Direct Radiation 13
2.3 AD-4B, AD-6, and AD-5 Test Aircraft 15
2.4 Pilot's Protective Thermal Hood 15
2.5 Modified APS-19 Radar Nacelle with Instrumentation Installed . . 16
3.1 Energy-versus-Time Curve, Shot 12, AD-5 20
3.2 Irradiance-versus-Time Curves, Shot 12, AD-5 20
3.3 Skin Temperature Time Histories, Shot 12, AD-5, Direct . . . 21
3.4 Skin Temperature Time Histories, Shot 12, AD-5, Ground-Reflected . 22
4.1 Airplane Position and Theoretical Ratios of Ground-Reflected to Direct Radiation, Shot 4, AD-6 25
4.2 Airplane Position and Theoretical Ratios of Ground-Reflected to Direct Radiation, Shot 4, AD-4B 26
4.3 Airplane Position and Theoretical Ratios of Ground-Reflected to Direct Radiation, Shot 6, AD-5 27
4.4 Airplane Position and Theoretical Ratios of Ground-Reflected to Direct Radiation, Shot 6, AD-6 28
4.5 Airplane Position and Theoretical Ratios of Ground-Reflected to Direct Radiation, Shot 8, AD-5 29
4.6 Airplane Position and Theoretical Ratios of Ground-Reflected to Direct Radiation, Shot 8, AD-4B 30
4.7 Airplane Position and Theoretical Ratios of Ground-Reflected to Direct Radiation, Shot 8, AD-6 31
4.8 Airplane Position and Theoretical Ratios of Ground-Reflected to Direct Radiation, Shot 12, AD-6 32
4.9 Airplane Position and Theoretical Ratios of Ground-Reflected to Direct Radiation, Shot 12, AD-5 33
4.10 Airplane Position and Theoretical Ratios of Ground-Reflected to Direct Radiation, Shot 12, AD-4B 34
4.11 Airplane Position and Theoretical Ratios of Ground-Reflected to Direct Radiation, Shot 13, AD-4B 35
4.12 Airplane Position and Theoretical Ratios of Ground-Reflected to Direct Radiation, Shot 13, AD-5 36
4.13 Measured versus Calculated Direct Energy Data 38
4.14 Measured versus Calculated Indirect Energy Data 39
4.15 Energy per Kiloton versus Slant Range 39
4.16 Normalized Irradiance and Generalized Field Pulse versus Time, Shot 4 40
4.17 Normalized Irradiance and Generalized Field Pulse versus Time, Shot 6 41
4.18 Normalized Irradiance and Generalized Field Pulse versus Time, Shot 8 42
4.19 Normalized Irradiance and Generalized Field Pulse versus Time, Shot 12 43
4.20 Normalized Irradiance and Generalized Field Pulse versus Time, Shot 13 44
4.21 Energy versus Skin Temperature Curves (Quartz Filter) 45

4.22 Energy versus Skin Temperature Curves (No Filter) 46
4.23 Temperature Rise versus Energy Curves 47
4.24 Temperature Rise times Slant Range versus Total Yield Curves (Quartz Filter) 48
4.25 Temperature Rise times Slant Range versus Total Yield Curves (No Filter) 49

TABLES

3.1 Summary of Direct and Ground-Reflected Data 19
4.1 Percent of Total Direct and Ground-Reflected Filtered Energies . . 37
A.1 Summary of Direct Energy Data Computations 51
A.2 Summary of Ground-Reflected Energy Data Computations 51

Chapter I
INTRODUCTION

1.1 GENERAL

Thermal radiation is one of the primary effects produced by a nuclear detonation. Thermal radiation becomes the prime consideration for some aircraft weapon systems in the determination of criteria for safe delivery of nuclear weapons when the yield exceeds about 30 kilotons, and definitely becomes a more important factor for high yield weapons. Therefore, it is necessary to determine the various factors which constitute the spatial and temporal variation of thermal radiation and the mechanism by which the thermal radiation produces a resultant temperature increase in aircraft components.

The basic factors are: (1) the quantity of thermal radiation produced as a function of yield, (2) the time dependence of thermal emission, (3) spectral distribution, (4) the scattered and reflected radiation which augments the direct radiation, and (5) the atmospheric attenuation of the radiation. To date much data has been accumulated in References 1 and 2 The total thermal energy produced for an air burst is given by Y (cal) = $0.44\ 10^{12}W^{0.84}$ where W is the total yield in kilotons. The radiant power consists of two maxima where the time to the second $t_{max} = 0.032\ W^{1/2}$ where t_{max} is in seconds when W is expressed in kilotons. For surface bursts and near surface bursts the quantity and time-picture is incomplete until an air burst in the megaton range is performed for comparative purposes. In Reference 3, the effect of the distorted fireball on thermal yield is discussed. However, more knowledge of the spectral and spatial distributions, particularly in the infrared region during the second pulse for all conditions of burst, was necessary. This information was required to determine (1) the reflection coefficient of the ground surface, since this coefficient has a spectral dependence, and (2) the absorption coefficient of the aircraft skin surface. Much data has been available on the spectral distribution of direct radiation; however, no data was available on the reflected radiation. Some data had been accumulated on the scattered radiation and attenuation (see Reference 4 and its bibliography), but considerable work still remained. No complete experimental program had been executed on reflected radiation from a nuclear detonation. To limit the effort and fill the largest gap, this program was undertaken.

The only extensive theoretical predictions for reflected radiation for a homogeneous absorbing but nonscattering atmosphere were available in Reference 5; however, recent calculations with greater numerical accuracy have been performed at the National Bureau of Standards, using the S. E. A. C. computer under Armed Forces Special Weapons Project sponsorship, and at the Douglas Aircraft Corporation on the IBM MK-701 computer. The latter two are self-consistent. In all instances a point source was assumed along with an infinite reflecting plane obeying Lambert's law. These particular calculations were for the case of a 2π steradian receiver oriented parallel to the reflecting plane. Additional calculations were also performed by the Douglas Aircraft Corporation for the specific cases of interest here. These were: (1) 90-degree-field-of-view receiver oriented toward the fireball and (2) 90-degree-field-of-view receiver with surface of the sensing element parallel to the earth's surface. These calculations were required to determine the degree of validity of the theoretical predictions.

1.2 PROJECT OBJECTIVES

The specific objectives of this project were:

1. To study the direct and ground-reflected components of thermal radiation by measuring that radiation received at different points in space relative to the burst by means of 90-degree-field-of-view calorimeters aimed directly at the fireball and ground directly below the test aircraft. These measurements were required as an experimental check on the analytical data contained in Reference 5. These analytical data have been used as one of the bases for establishing effects envelopes for the safety of atomic weapon delivery tactics employed by the Fleet. These criteria are contained in Reference 6.

2. Since the reflected radiation may have a spectral dependence different from the direct radiation as a consequence of selective absorption by the reflection plane, measurements on the spectral composition of both the direct and reflected components as recorded by 90-degree-field-of-view calorimeters aimed directly at the fireball and the ground below the test aircraft were performed.

3. To obtain time-histories of the temperature rise and decay in aircraft skin specimens, exposed to and shielded against the effects of aerodynamic cooling. These data are required to supplement similar data obtained by Project 5.1 during Operation UPSHOT-KNOTHOLE.

Chapter 2
EXPERIMENT DESIGN

2.1 BACKGROUND AND THEORY

2.1.1 Thermal Radiation. Aircraft flying in the vicinity of an atomic explosion are subjected to the following major weapon effects: gamma radiation, thermal radiation, gust loading, and shock overpressure. These effects are of primary significance in the establishment of techniques and procedures to be utilized in the delivery of atomic weapons.

The test result obtained by Project 5.1 during UPSHOT-KNOTHOLE (Reference 7) clearly demonstrated that as much as 40 percent of the total thermal radiation received by aircraft in flight was due to ground reflection of the incident radiation. Similar data have also been obtained during other experimental tests (Reference 2). In order to establish reliable thermal effects criteria, the amount of reflected thermal radiation to be received at various points in space about the burst center under different conditions must be predictable within reasonable limits. Analytical procedures and methods for accomplishing this have already been developed (Reference 5). The data have been utilized as one of the bases for establishing the thermal radiation effects criteria as included in the present U. S. Navy Effects Handbook (Reference 6). All the effects criteria and guides governing the safety of atomic weapon delivery tactics employed by the fleet are contained in this handbook.

As presented in Reference 6, the radiant energy (direct and reflected) received in space, assuming a nonscattering homogeneous atmosphere, is given by the expression:

$$E = \frac{W_{th}\left[1 + E_{z_r}/E_{z_d}\right]\cos i\ (e^{-\alpha R})}{4\pi R^2} \qquad (2.1)$$

Where: E = total energy in cal/cm^2
W_{th} = thermal source in calories
$\cos i$ = cosine of angle between radius vector for source to receiver and the normal to the receiver
α = atmospheric attenuation coefficient
R = slant range distance in centimeters
E_{z_r} = ground reflected energy from an infinite plane
R_{z_d} = direct energy normal to receiving surface

The bracketed expression represents the increase to the direct radiation due to reflection, provided the appropriate value for E_{z_r}/E_{z_d}, which is a function of the orientation of the receiver, is available. In the event that the receiver is parallel to the ground and has a 2-steradian field of view, generalized curves are available in Reference 5 which permit the determination of the theoretical values of $\beta^{-1}(E_{z_r}/E_d)$, where β is the surface reflection coefficient for all spatial locations of interest. For the particular burst heights employed here, namely 300 and 500 feet, the individual curves are shown in Figures 2.1 and 2.2. The ratio E_{z_r}/E_d is then obtained directly by multiplying by the

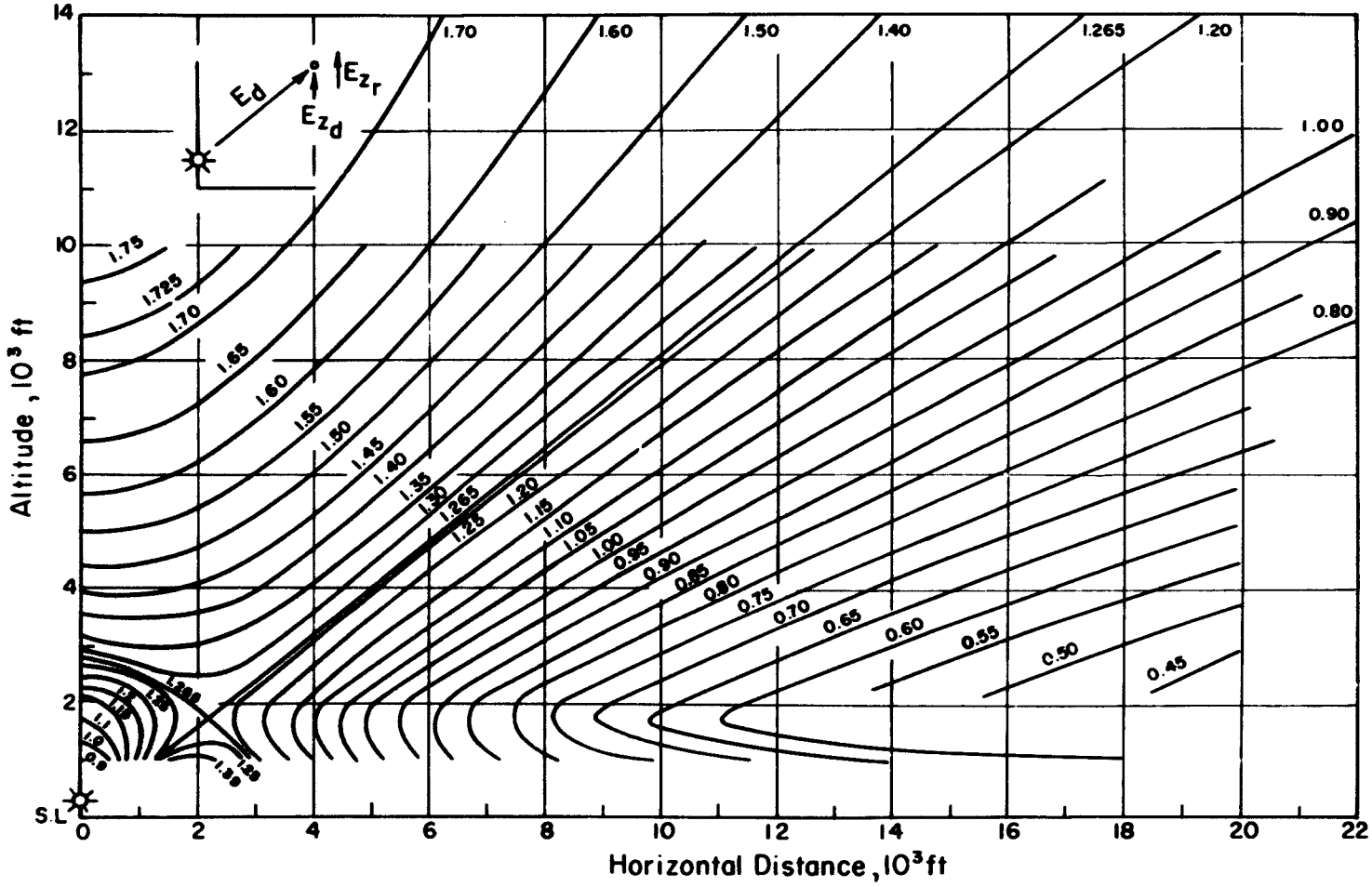

Figure 2.1 Ratio of Reflected to Direct Radiation. Explosion at 300 feet above Diffuse Infinite Plane. Reflectivity of Surface = 100 percent. Note: Values shown are the ratio of vertical components of the reflected to the vertical component of direct radiation (E_{z_r}/E_{z_d}).

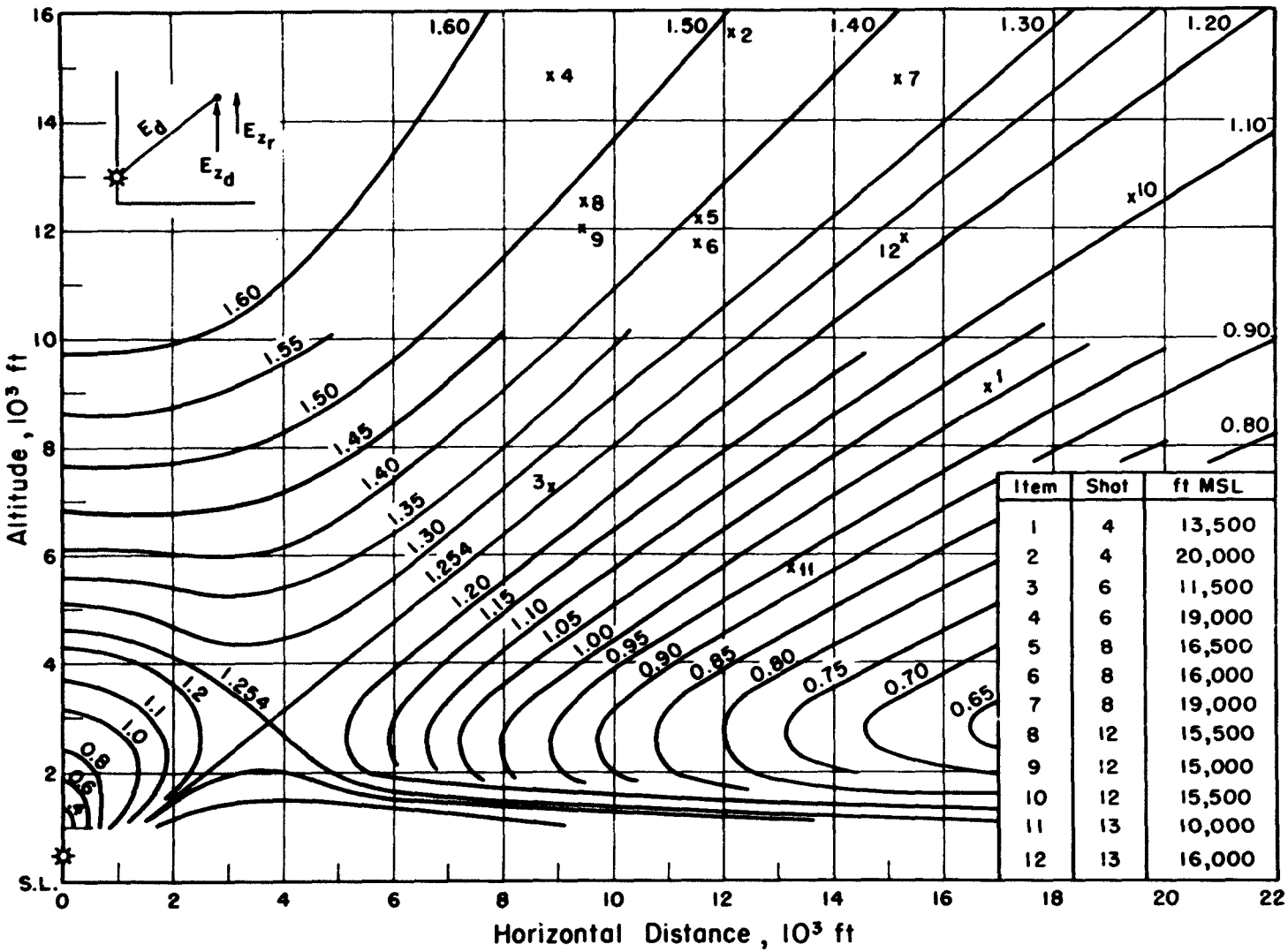

Figure 2.2 Ratio of Reflected to Direct Radiation. Explosion at 500 feet above Diffuse Infinite Plane. Reflectivity of Surface = 100 percent. Note: Values shown are the ratio of vertical components of the reflected to the vertical component of direct radiation (E_{z_r}/E_{z_d}).

appropriate value of β for the particular reflecting surface under consideration. Some typical values of β are given in Reference 6, pages 3-16 and 3-17. The reader is referred to Reference 5 for the theoretical development of reflected radiation received by a receiver parallel to an infinite reflecting plane and also when normal to the radius vector through the source.

2.1.2 Temperature Rise in Aircraft Skin Panels. Measurements of the maximum temperature rise attained to date in the metal skin of the test aircraft were made by Project 5.1 during UPSHOT-KNOTHOLE. The majority of such measurements were made using passive type thermal indicators (temperature tapes). A limited number of time-histories of the temperature rise in skin specimens were obtained using temperature gages. The data obtained from these measurements are contained in Reference 7. In general, the application of temperature tapes exhibited definite limitations, and the data obtained could not be consistently correlated with measured thermal inputs and visible thermal damage. Additional skin panel temperature-time data are required to supplement the data previously obtained before a complete evaluation and correlation of all data can be made.

As presented in Reference 6, the maximum temperature rise in aircraft metal skin exposed to thermal radiation, without cooling, is given by:

$$(T_M - T_A) = \frac{\gamma E}{\rho C_{pt}} \qquad (2.2)$$

Where: T_M = maximum allowable skin temperature (°F)
T_A = ambient air temperature (°F)
E = thermal input as defined by Equation 2.1
ρ = specific density of material
C_p = specific heat of material
t = thickness of material (ft.)
γ = thermal absorption coefficient (non-dimensional)

Considering the effects of aerodynamic cooling the maximum temperature rise is given by:

$$(T_M - T_A) = \frac{F\gamma E}{\rho C_p t} \qquad (2.3)$$

where F is the convective cooling factor dependent upon air speed, altitude and time of irradiance of the receiver. (See Reference 6 for a complete discussion).

2.1.3 Spectral Composition of Direct and Reflected Radiation. Information is required concerning the spectral composition of the reflected component of thermal radiation to ascertain which (if any) wave lengths of bands of the spectrum are absorbed by the reflecting surface. By comparison with the spectral composition of the direct radiation, certain portions of the spectrum may be shown to have a direct relationship to the thermal damage experienced by different type surface finishes.

2.2 TEST PROCEDURES AND CONDITIONS

Three instrumented model AD type aircraft, Figure 2.3, participated in Shots 4, 6, 8, 12, and 13 of Operation TEAPOT. One of the three AD aircraft served primarily as a standby aircraft, except during Shots 8 and 12 when records were obtained with all three

Figure 2.3 AD-4B, AD-6, and AD-5 Test Aircraft.

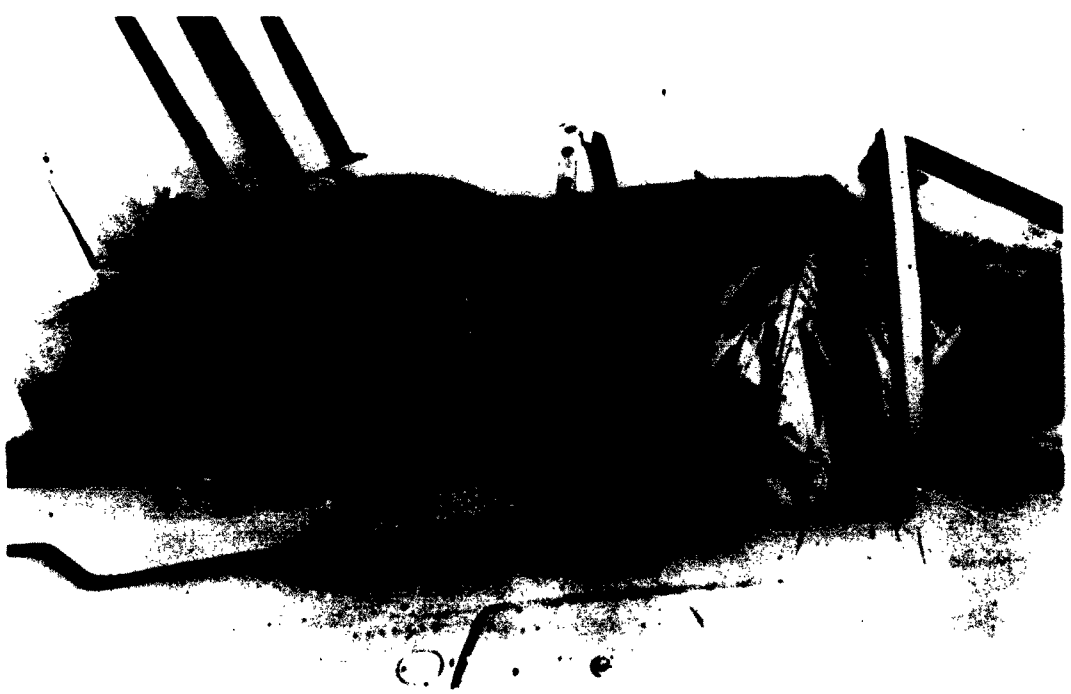

Figure 2.4 Pilot's Protective Thermal Hood.

Figure 2.5 Modified APS-19 Radar Nacelle with Instrumentation Installed.

aircraft. During each shot, test aircraft were flown at approximately 175 knots indicated air speed (IAS) in counter-clockwise orbits about ground zero, initiating standard-rate break-away turns after detonations. Utilizing a thermal hood over the cockpit, Figure 2.4, and special goggles for pilot's protection against thermal radiation, one or two test aircraft were monitored by MSQ-1 ground radar control and instrument flight rules. Since MSQ-1 control was only available for one or two aircraft, when two or three test aircraft participated, the third and at times the second aircraft flew formation on the monitored aircraft with visual flight rules except for the period of the initial flash during which time the thermal hood was in place and instrument flight rules prevailed. Each aircraft was assigned to fly at a different altitude and horizontal range (radius of orbit) from ground zero. At T-20 seconds the instrumentation recording equipment in each aircraft was turned on by the pilot. At approximately T+2 seconds the pilot executed a standard rate turn to the outside of the orbit in order to receive the subsequent shock wave in a near "tail-on" position. Each aircraft was instrumented to measure and record the following data at time zero: (1) the direct and reflected components of thermal radiation received at the aircraft position in space, (2) the time-history of the temperature rise in exposed aircraft skin specimens, and (3) the spectral composition of the direct and reflected components of thermal radiation.

The aircraft test positions for each of the shots are shown in Figure 2.2. Test positions were selected which would give the maximum possible distribution of data points with respect to the burst center. From such data experimental check E_{z_r}/E_{z_d} curves similar to those shown on Figures 2.1 and 2.2 could be made.

2.3 INSTRUMENTATION

2.3.1 General Arrangement. Each test aircraft was equipped to carry a modified APS-19 radar nacelle which was mounted on the underside of the port wing on the wing bomb rack, as shown in Figure 2.5. All radar gear was removed from the nacelle. The nacelle, or tank, was modified to carry all the instrumentation measuring and recording equipment. During tests, all equipment was turned on by means of a switch in the cockpit of the aircraft. The instrumented nacelles could be readily installed or removed from the test aircraft for maintenance, servicing, or repair of test equipment.

Essentially, two similar sets or banks of measuring instruments were carried in each tank. Each set or bank of instruments consisted of four Naval Radiological Defense Laboratory (NRDL) disc-type calorimeters and one NRDL foil-type radiometer, six aircraft skin-panel temperature specimens, and two 16-mm gun-sight-aiming-point (GSAP) gun cameras. Each bank of instruments was mounted in the tank in such a manner that, as the test aircraft flew in a circular orbit (counterclockwise) about ground zero, one bank looked at the burst point and the other bank looked at the ground immediately below the test aircraft. The position of each bank of instruments in the tank could be adjusted on the ground to maintain the above reference, depending upon the planned position of the aircraft for the particular test.

2.3.2 Instrumentation Equipment. NRDL disk-type calorimeters and foil-type radiometers having a 90-degree field of view were used for measuring thermal radiation. Quartz filters, having a transmissivity of 92 percent, were used on two calorimeters and one radiometer of each bank of instruments for measurements of total radiation. Yellow, and red filters having a transmissivity of 90 and 88 percent, respectively, were used on the other two calorimeters for spectral measurements. Sixteen-millimeter GSAP gun cameras were also used to photograph and check the alignment and field of view of the calorimeters during the test and to provide a basis for correcting calorimeter data readings which were "off target."

Thermocouples attached to the aft side of aluminum skin specimens ($1\frac{3}{4}$-inch diameter specimens, 0.016 inch thick, having various surface finishes) were used for obtaining temperature-time histories. On some tests the surfaces of these specimens were exposed to the airstream; on some other tests, quartz filters were used to shield the specimens against airstream cooling effects.

A further description of the instrumentation is presented in Reference 8.

Chapter 3
RESULTS

Direct and ground-reflected calorimeter, radiometer, and skin sample temperature time-history recordings were obtained for 12 different test positions during Operation TEAPOT. A summary of peak recordings with aircraft test positions during Shots 4, 6, 8, 12, and 13 is presented in Table 3.1. Typical time-history plots for each of the above parameters are presented in Figures 3.1 to 3.4. All direct and ground-reflected recordings were incident on sensing elements of 90-degree-field-of-view calorimeters and radiometers. Aircraft positioning data shown in Table 3.1 were determined from MSQ-1 radar plot board data.

3.1 CALORIMETER DATA

Calorimeter data were read directly from oscillograph records by means of a telereader. Proper thermal and electric calibration constants, calorimeter disk heat loss and filter transmissivity corrections were applied. Gun camera records of fireball and ground directly below test aircraft showed that aiming corrections to recorded values was unnecessary. Calorimeter data recorded by oscillograph Channels 4 and 7 represent total direct and ground-reflected energies under clear quartz filter, while data recorded by Channels 5 and 8 represent energies under yellow (3-69) and red (2-58) Corning filters. Respective spectral ranges for these filters were 2,200–45,000; 5,300–25,000; and 6,400–25,000 Å as shown in Reference 2.

3.2 RADIOMETER DATA

Radiometer data were reduced by the same method applied to calorimeter data, except no heat loss correction was applied. Oscillograph Channel 6 recorded irradiance under clear quartz filter. Peak values and time to second maximum are presented in Table 3.1.

3.3 SKIN SAMPLE TEMPERATURE DATA

Skin sample temperature data were reduced by the same method applied to radiometer data. Oscillograph Channels 1, 2, and 3 recorded temperatures of bare, white, and blue painted 1¾-inch-diameter, 0.016-inch-thick aluminum skin samples exposed to the airstream. Channels 10, 11, and 12 recorded temperatures of the same skin samples, respectively, but shielded against the airstream by clear quartz filters. Maximum recorded temperatures in all skin samples (both exposed to and shielded against the free airstream) are shown in Table 3.1 for all test conditions. Typical time-histories of temperature rise and decay in exposed and shielded skin samples are shown in Figures 3.3 and 3.4.

TABLE 3.1 SUMMARY OF DIRECT AND GROUND REFLECTED DATA

TEAPOT Event				Shot 4				Shot 6				Shot 8			
Date of Test				7 March 1955				22 March 1955				29 March 1955			
Yield (KT)				43 ± 2				8.1 ± 0.2				15 ± 2			
Item				(1)		(2)		(3)		(4)		(5)		(6)	
Test Aircraft				AD-6		AD-4B		AD-5		AD-6		AD-5		AD-4B	
Bureau Number				134613		132255		133880		134613		132848		132255	
Aircraft Altitude (feet MSL)				13,500		20,000		11,500		19,000		16,000		16,000	
Aircraft Altitude above Burst (feet)				8,510		15,010		6,755		14,255		11,690		11,190	
Aircraft Horizontal Range (feet)				16,000		12,200		8,925		8,900		11,600		11,600	
Aircraft Slant Range (feet)				18,000		19,350		11,200		18,000		16,450		16 100	
Aircraft Positioning Method				Navy MSQ		AF MSQ		Navy MSQ		AF MSQ		Navy MSQ		Form on AD-5	
Maximum direct and ground reflected calorimeter, radiometer, and skin temp. measurements				Direct	Ground Reflect	Direct	Ground Reflect	Direct	Ground Reflect	Direct	Ground Reflect	Direct	Ground Reflect	Direct	Ground Reflect
Disks	Chan. No	Units	Filter (Transmissivity - pct)												
Calorimeter	(4)	cal/cm²	Clear Quartz (92)	4.19	0.33	3.97	3.15	2.13	0.53	1.36	0.53	2.24	1.41	2.06	1.44
Calorimeter	(7)	cal/cm²	Clear Quartz (92)	3.84	0.33	3.81	2.79	2.07	0.34	1.13	1.06	1.85	1.31	2.13	1.31
Calorimeter	(5)	cal/cm²	Yellow 3-69 (90)	2.02	0.30	3.03	2.55	1.77	0.60	0.76	0.77	1.27	1.02	1.53	1.25
Calorimeter	(8)	cal/cm²	Red 3-58 (60)	2.38	0.30	2.38	1.84	1.31	0.42	No defl.	0.53	1.04	0.51	1.22	1.02
Radiometer	(6)	cal/cm²/sec.	Clear Quartz (92)	5.90	No defl.	5.05	2.97	5.05	0.17	2.23	1.07	2.58	1.06	2.90	2.22
	(6)	sec.	Time to sec. max.	0.213	—	0.23	0.23	0.115	0.125	0.115	0.115	0.22	0.22	0.23	0.23
Bare Skin	(1)	°F.	None	41	21	30	23	34.1	12 7	17 6	No defl.	22	17.5	No defl.	17.5
White Skin	(2)	°F.	None	30	16	45	30	22.3	9.0	14.5	9.9	18	13.9	24.9	14.6
Blue Skin	(3)	°F.	None	118	45	116	109	76.1	33.3	44.4	34.9	66.5	42	66.6	59.9
Bare Skin	(10)	°F	Clear Quartz (92)	46.8	15.3	NG	30	33.6	16.0	21.6	16.1	25.5	16.3	40.2	21.1
White Skin	(11)	°F.	Clear Quartz (92)	30	12.5	24.2	23	23.5	No defl.	16.0	8.3	18.5	No defl.	18.9	17.6
Blue Skin	(12)	°F.	Clear Quartz (92)	103.5	32.6	134.5	103	76.8	31.4	54.5	30.4	66	33.8	76.5	57.5

TEAPOT Event				Shot 12				Shot 13							
Date of Test				15 April 1955				5 May 1955							
Yield (KT)				24				30 ± 2							
Item				(7)		(8)		(9)		(10)		(11)		(12)	
Test Aircraft				AD-6		AD-6		AD-5		AD-4B		AD-4B		AD-5	
Bureau Number				134613		134613		133880		132255		132255		133880	
Aircraft Altitude (feet MSL)				19,000		15,500		15,000		15,500		10,000		16,000	
Aircraft Altitude above Burst (feet)				14,190		12,695		11,525		12,025		5,205		11,205	
Aircraft Horizontal Range (feet)				15,100		9,500		9,500		10,000		12,200		15,200	
Aircraft Slant Range (feet)				20,750		15,500		14,900		22,500		14,200		19,900	
Aircraft Positioning Method				AF MSQ		Navy MSQ		Form. on AD-6		Form. on AD-6		AF MSQ		AF MSQ	
Maximum direct and ground reflected calorimeter, radiometer, and skin temp. measurements				Direct	Ground Reflect	Direct	Ground Reflect	Direct	Ground Reflect	Direct	Ground Reflect	Direct	Ground Reflect	Direct	Ground Reflect
Disks	Chan. No.	Units	Filter (Transmissivity - pct)												
Calorimeter	(4)	cal/cm²	Clear Quartz (92)	1.07	0.76	5.42	3.30	6.01	4.27	1.71	0.30	4.40	0.46	2.94	0.66
Calorimeter	(7)	cal/cm²	Clear Quartz (92)	1 10	0.63	4.90	3.72	5.08	3.70	1.91	0.30	4.16	0.57	2.70	0.59
Calorimeter	(5)	cal/cm²	Yellow 3-69 (90)	0.75	0.60	3.04	2.74	3.00	2.04	1.31	0.23	2.11	0.46	1.80	0.66
Calorimeter	(8)	cal/cm²	Red 3-58 (60)	No defl.	0.56	2.44	2.20	2.18	1.51	No defl.	0.20	2.54	0.44	1.77	0.46
Radiometer	(6)	cal/cm²/sec.	Clear Quartz (92)	1.57	1.02	7.55	6.46	9.0	6.1	3.20	No defl.	6.52	No defl.	3.60	No defl.
	(6)	sec	Time to sec. max.	0.23	0.20	0.180	0.20	0.180	0.205	0.18	—	0.22	—	0.215	—
Bare Skin	(1)	°F.	None	11.1	8.3	60	44	58	52	18	11.6	30.6	16.5	27.0	16.5
White Skin	(2)	°F	None	13.5	6.7	56	42	51	37	No defl.	8.7	30.4	13.8	23.0	16.7
Blue Skin	(3)	°F.	None	37.1	26.6	144.6	141.8	175	130.6	67.4	26.6	136	50	66.7	42.5
Bare Skin	(10)	°F	Clear Quartz (92)	19.7	10.0	79.3	49.8	73	54	20.2	10.7	72	15	30.0	15.5
White Skin	(11)	°F.	Clear Quartz (92)	16.2	4.2	43.6	41.9	50	43	19.9	4.2	42	13.2	27.1	9.0
Blue Skin	(12)	°F.	Clear Quartz (92)	46.5	26.1	154.6	122.5	170	111	72.5	24.2	147	36	66.5	34.6

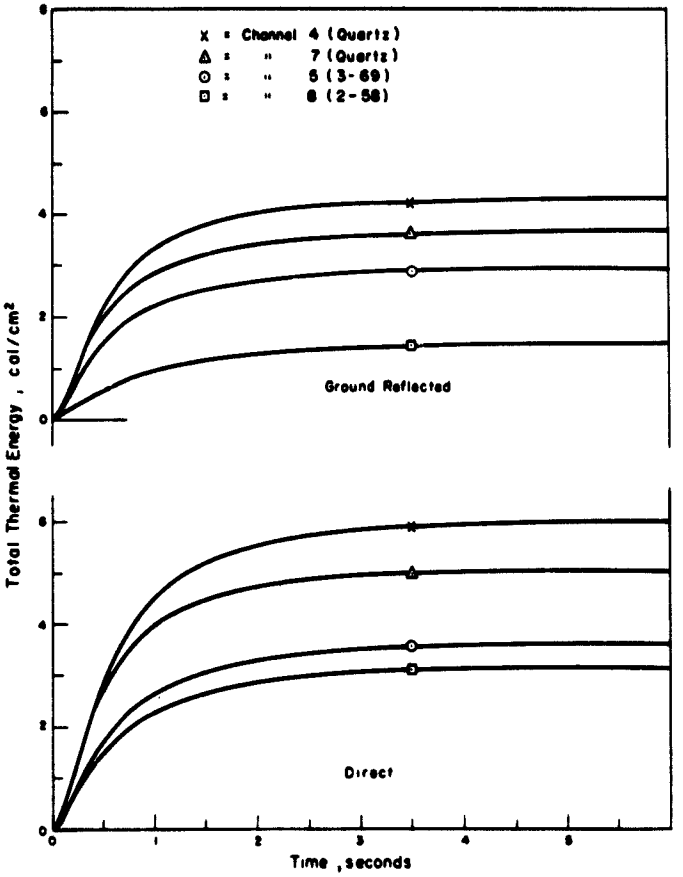

Figure 3.1 Energy-versus-Time Curve, Shot 12, AD-5.

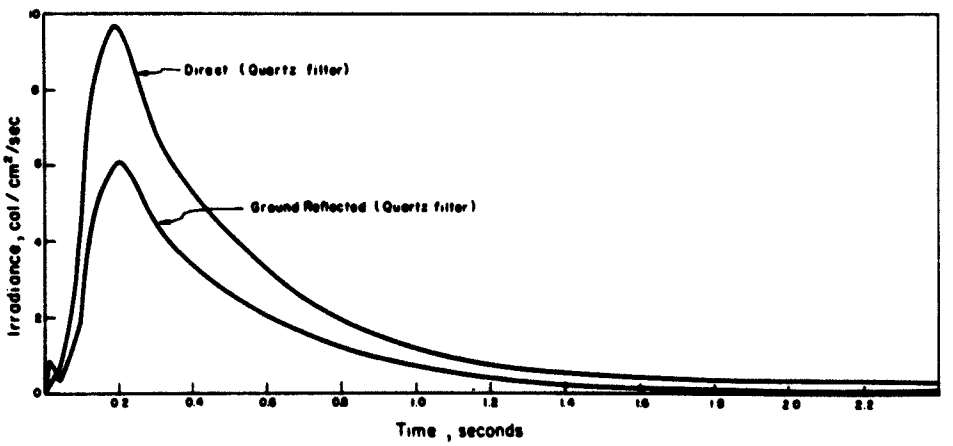

Figure 3.2 Irradiance-versus-Time Curves, Shot 12, AD-5.

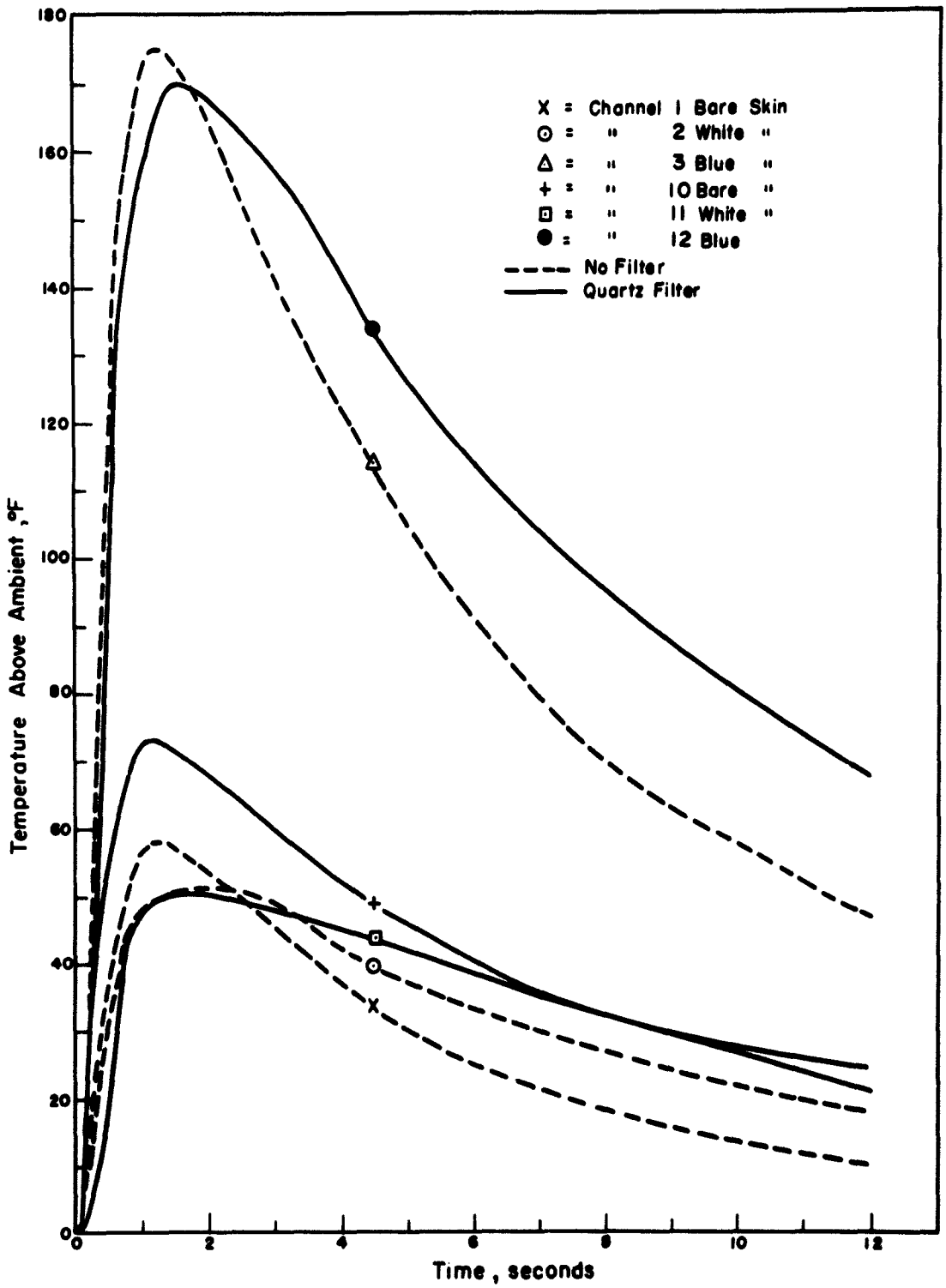

Figure 3.3 Skin Temperature Time Histories, Shot 12, AD-5, Direct.

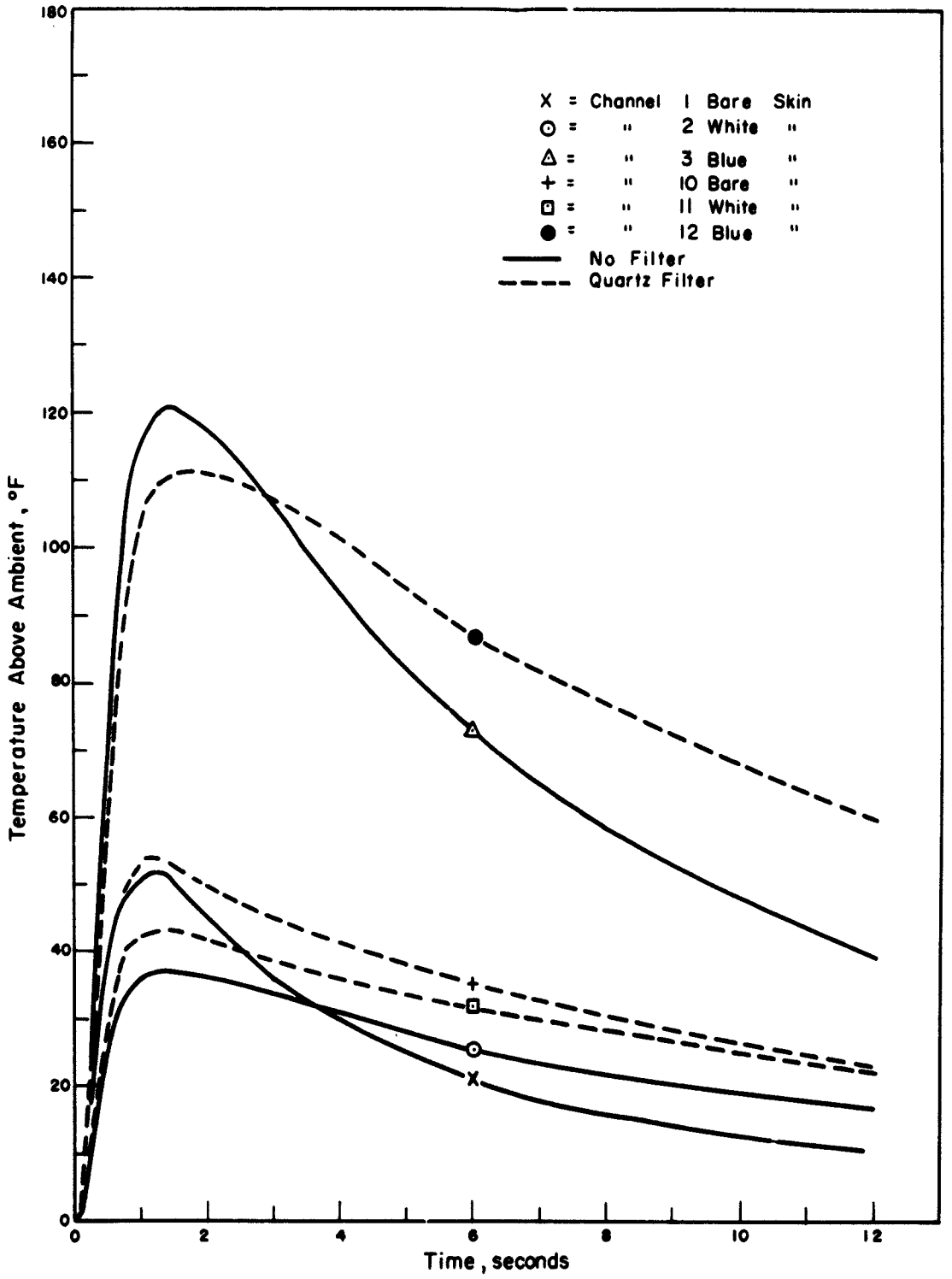

Figure 3.4 Skin Temperature Time Histories, Shot 12, AD-5, Ground-Reflected.

Chapter 4
DISCUSSION

4.1 EXPERIMENTAL CHECK ON ANALYTICAL DATA

4.1.1 General. The analytical approach to the problem of the quantity of reflected radiation received by a detector considered a nonscattering, nonabsorbing atmosphere where the reflecting plane was infinite in extent. The experiment conducted here obviously did not satisfy this ideal model and therefore the reduction of the data entailed considerable analysis. Specifically, the reflected radiation received by the instrumentation installed to observe direct radiation had to be subtracted, and conversely, the so-called indirect instrumentation at times received direct radiation. In either case, only finite areas of the reflecting plane were observed. Also, the observations were made in a real atmosphere where attenuation and scattering existed, thus requiring suitable corrections for these factors. The method of data reduction and results are presented below.

4.1.2 Data Reduction Procedure. The total energy received by an airborne receiver with a solid angle larger than the solid angle subtended by the fireball will consist of direct, reflected, and scattered radiation, where the contribution of each to the total will differ with spatial location and aiming direction. Here the aiming directions were either (1) through air zero (direct) or (2) normal to ground (indirect). Each case will now be considered.

1. Direct Radiation. The radiation measured on the direct calorimeter, E_{dm}, can be defined by the expression:

$$E_{dm} = E_d^* \left[1 + \beta \frac{E_r}{E_d} \kappa + \frac{E_s}{E_d^*} \right] \tag{4.1}$$

Where: E_d^* = contribution of the radiation emitted by the fireball proper
E_r = total reflected radiation
E_s = scattered radiation
E_d = direct radiation in vacuo defined by $W_{th}/4\pi R^2$
R = slant range
κ = attenuation correction to the reflected radiation

The value of β for the Nevada Proving Grounds has been determined to be 0.40. The value for κ has been approximated in the following fashion. The atmospheric transmissivity for the participating shots were given as 95 percent per nautical mile, and the average ratio of length of the path transversed by the rays of the reflected to the direct radiation is approximately 1.5, hence:

$$\frac{E_r\,(0.95)^{1.5n}}{E_d\,(0.95)^n} = \frac{E_r}{E_d}(0.95)^{0.5n} = \frac{E_r}{E_d}\kappa \tag{4.2}$$

where n is the slant range in miles. Replacing κ by its value in Equation (4.2), we can write (4.1) as

$$E_{dm} = E_d^* \left[1 + 0.40 \frac{E_r}{E_d} (0.95)^{0.5n} + \frac{E_s}{E_d^*} \right] \tag{4.3}$$

To determine E_d^*, the computed values of E_r/E_d were employed where

$$\frac{E_r}{E_d} = \frac{E_{zr}}{E_d} \cos i + \frac{E_{rr}}{E_d} \sin i \tag{4.4}$$

The numerical values of E_{zr}/E_d and E_{rr}/E_d for each shot are given in Figures 4.1 to 4.12. E_{zr} and E_{rr} are the vertical and horizontal reflected energy components, respectively, and "i" the angle of incidence of the direct radiation to indirect calorimeter. (See diagrams).

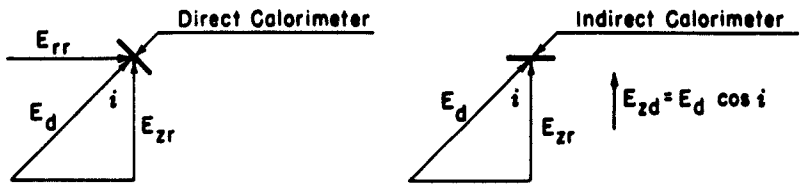

The values for E_s/E_d^* are computed in Reference 9 for a 4π receiver and single scattering. However, field-of-view measurements during the past several operations indicate that all but 10 percent of the total energy is received by a 90-degree-field-of-view detector. With this correction, the values of E_s/E_d^* for slant ranges considered are 0.05 to 0.07. To simplify the data reduction, a fixed value of 0.05 was taken. On substitution of the appropriate values into the bracketed expression, the value of E_d^* was obtained, and on dividing E_d^* by the direct transmissivity $(0.95)^n$ the in vacuo value of the direct radiation E_d was obtained.

2. Indirect Radiation. In a similar manner the radiation illuminating the indirect calorimeter can be expressed as:

$$E_{ind} = E_d^* \left[\cos i + \beta \frac{E_{zr}}{E_d} (0.95)^{0.5n} + \frac{E_s}{E_d^*} \right] \tag{4.5}$$

The above symbols have been defined previously. To determine E_{ind}, the values of E_d^* found above were employed and the analytical values of E_{zr}/E_d in Figures 4.1 to 4.12. For close-in stations where the indirect calorimeter included the fireball, a fixed value of $E_s/E_d^* = 0.05$ was taken. For the further-out station where E_d^* decreased, the value of E_s/E_d^* became larger, since E_s was unaffected. Finally, when the indirect calorimeter did not include the fireball and the direct radiation was large, the contributions from scattering would tend to increase the fractions. Considerable scattering in dust-laden air at the quite low aircraft altitudes apparently was received by the calorimeter. In this instance the value of $E_s/E_d^* \approx 0.15 \pm 0.05$. For this analysis a fixed value of 0.15 was assumed. The cos i term was dropped, since the normal component of direct radiation received by the indirect calorimeter was considered nil.

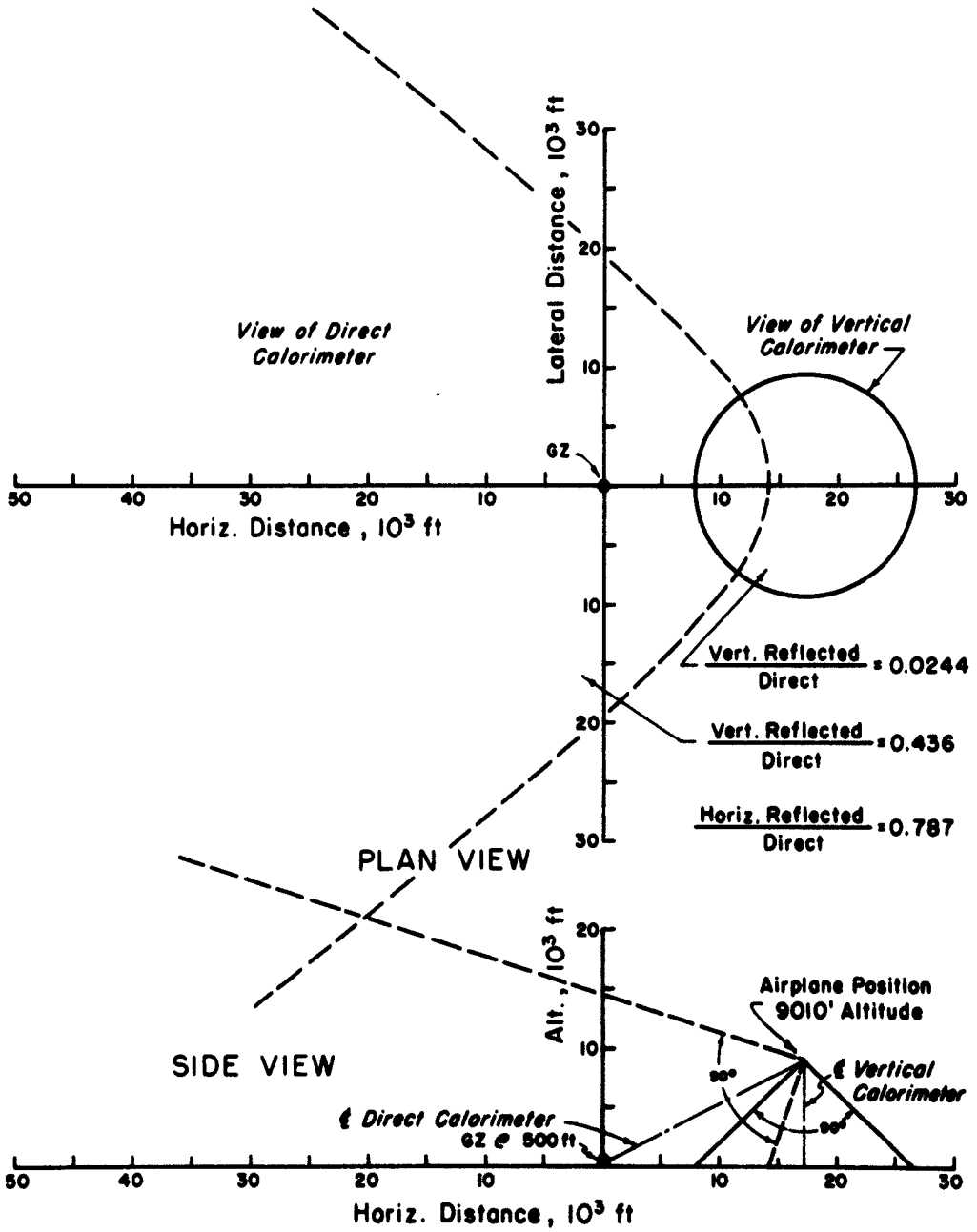

Figure 4.1 Airplane Position and Theoretical Ratios of Ground-Reflected to Direct Radiation, Shot 4, AD-6.

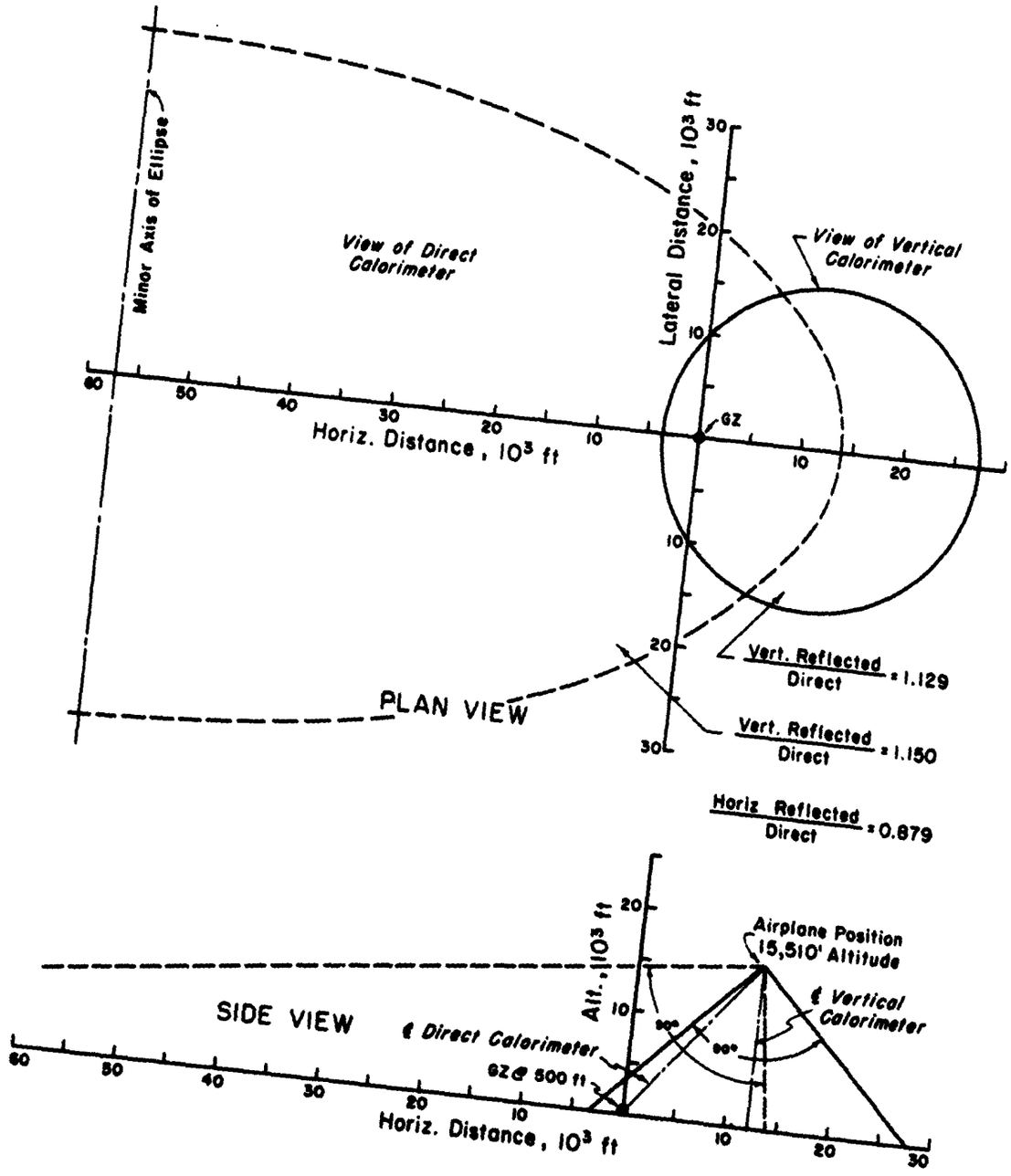

Figure 4.2 Airplane Position and Theoretical Ratios of Ground-Reflected to Direct Radiation, Shot 4, AD-4B.

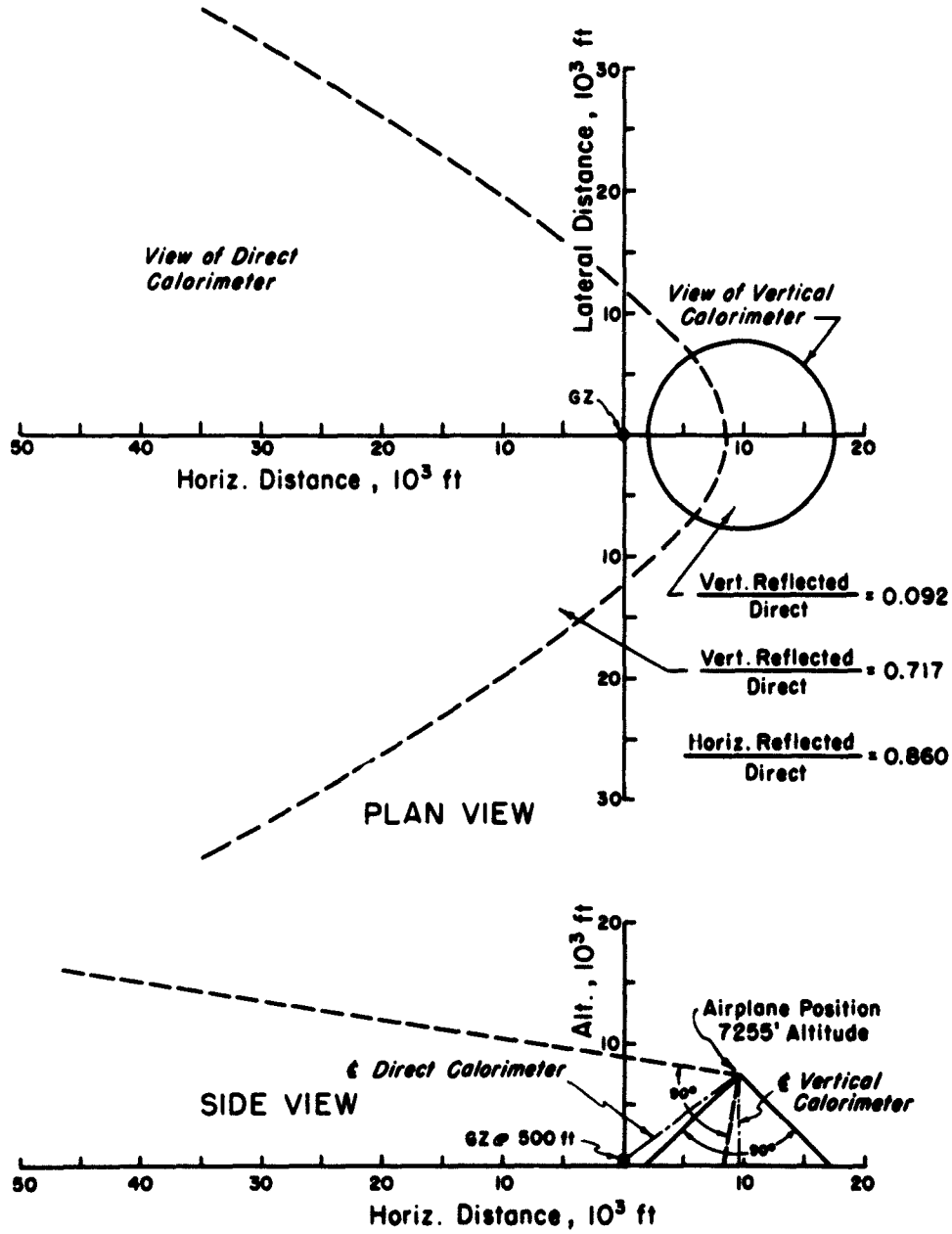

Figure 4.3 Airplane Position and Theoretical Ratios of Ground-Reflected to Direct Radiation, Shot 6, AD-5.

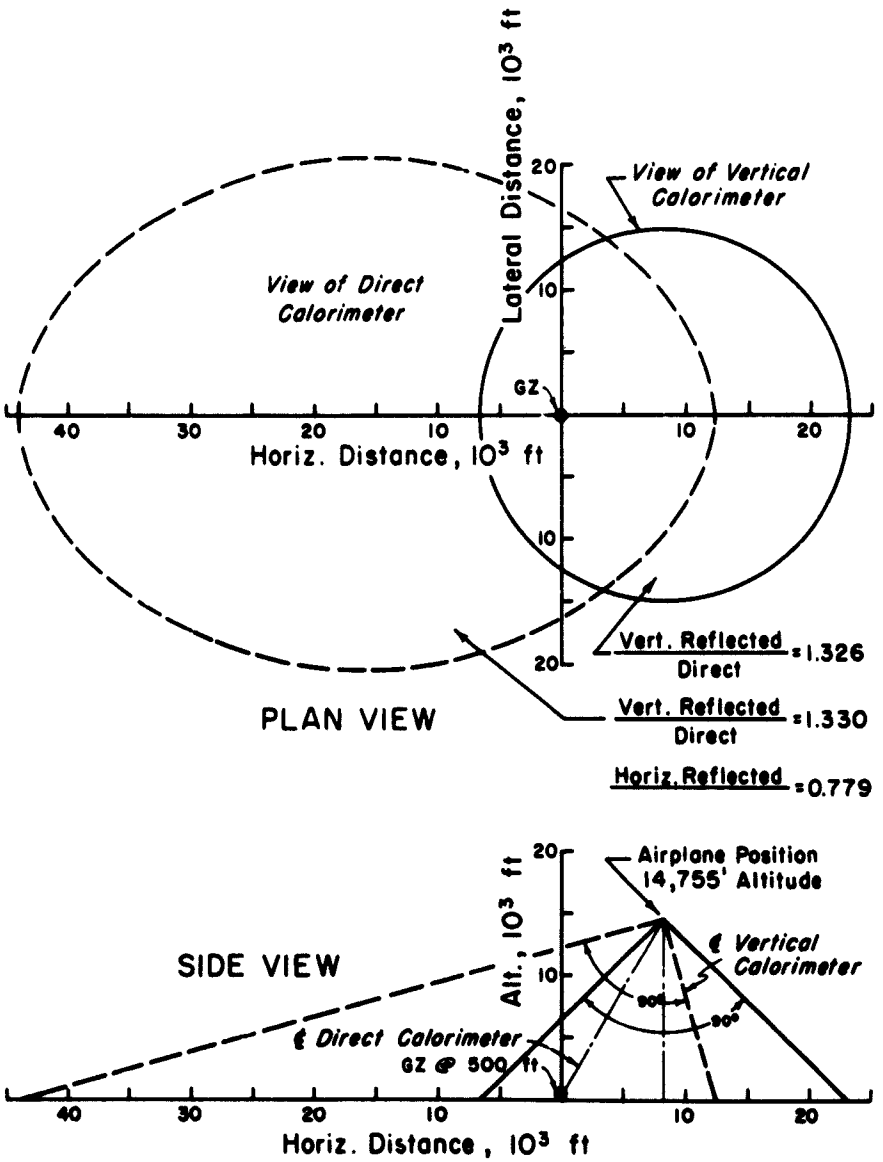

Figure 4.4 Airplane Position and Theoretical Ratios of Ground-Reflected to Direct Radiation, Shot 6, AD-6.

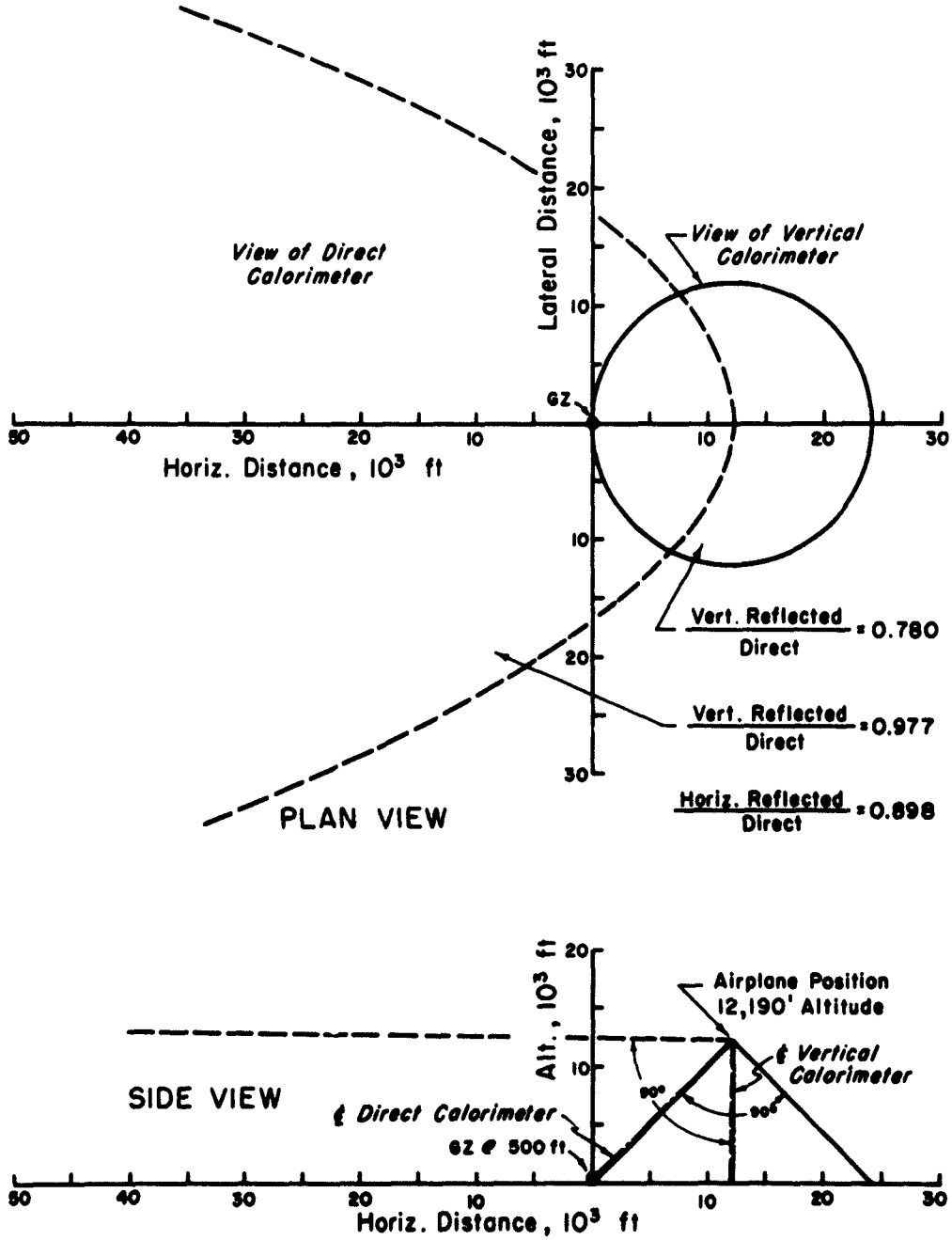

Figure 4.5 Airplane Position and Theoretical Ratios of Ground-Reflected to Direct Radiation, Shot 8, AD-5.

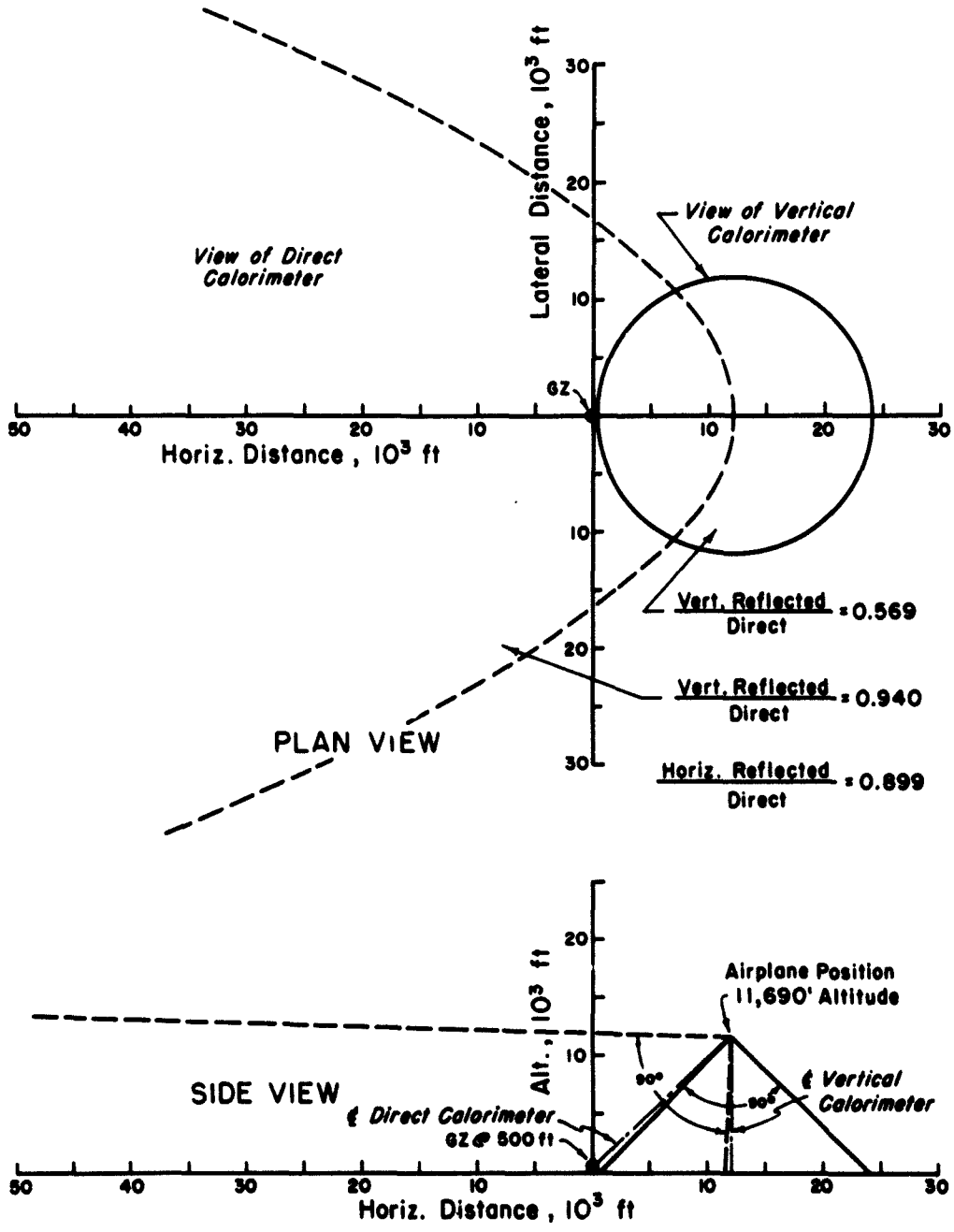

Figure 4.6 Airplane Position and Theoretical Ratios of Ground-Reflected to Direct Radiation, Shot 8, AD-4B.

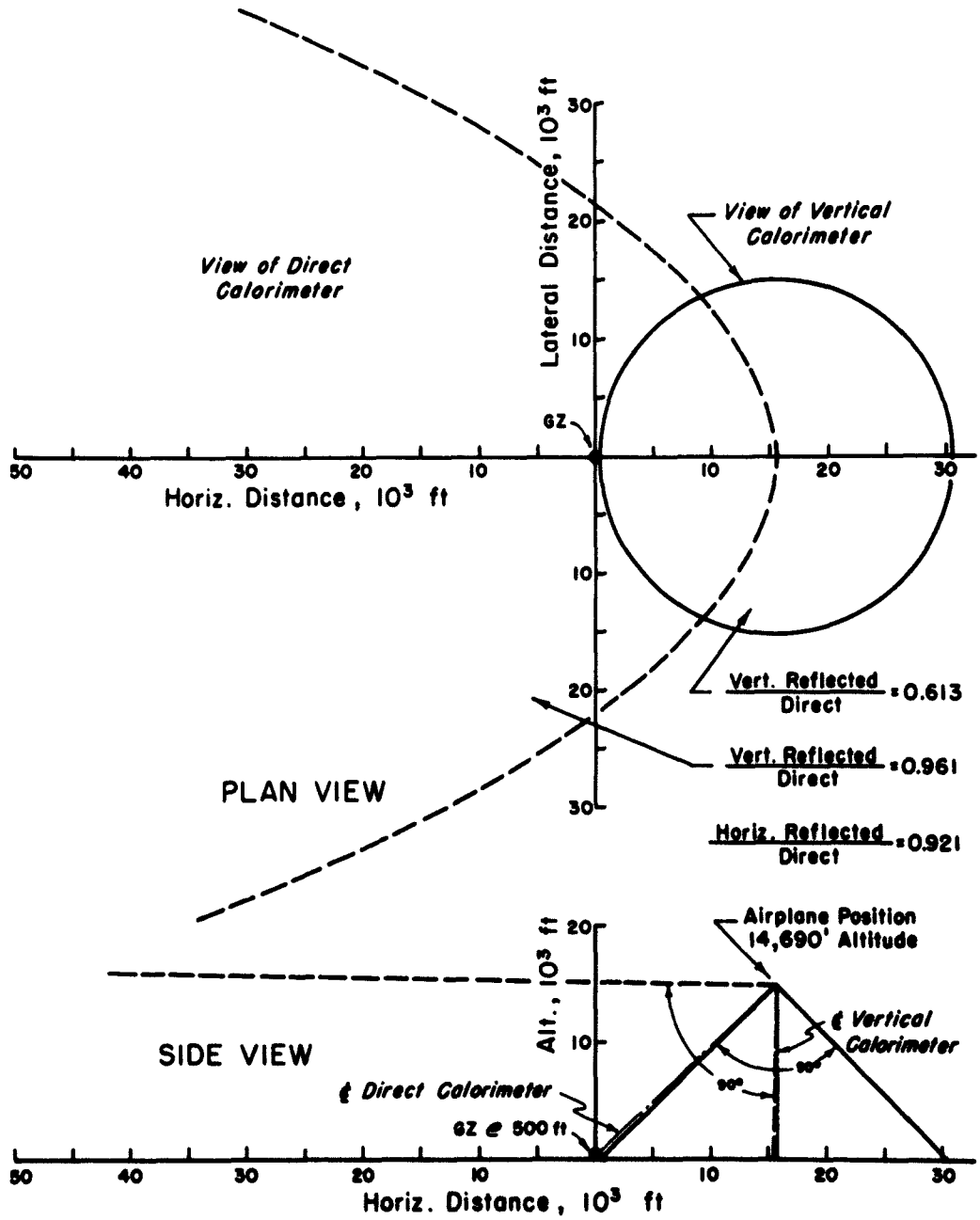

Figure 4.7 Airplane Position and Theoretical Ratios of Ground-Reflected to Direct Radiation, Shot 8, AD-6.

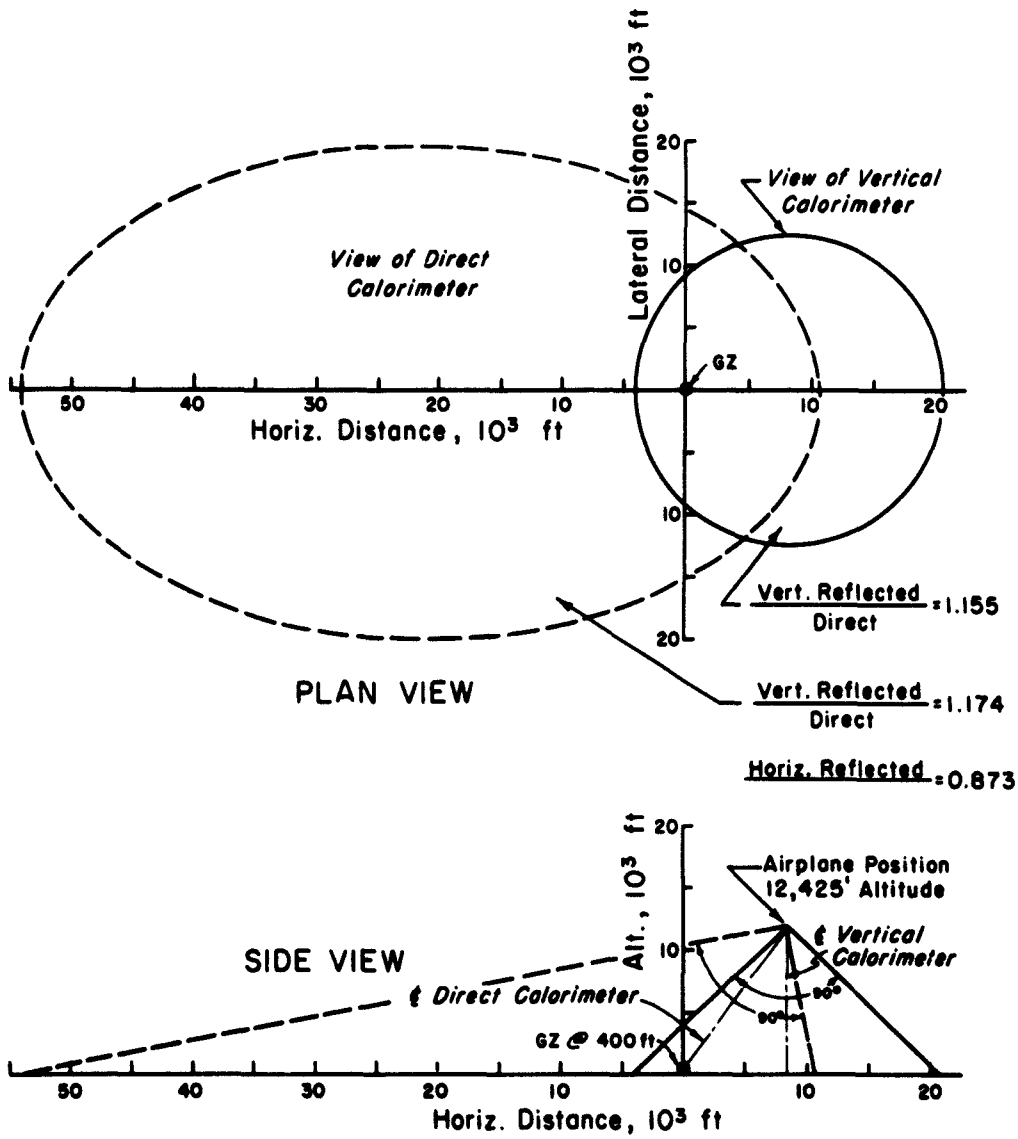

Figure 4.8 Airplane Position and Theoretical Ratios of Ground-Reflected to Direct Radiation, Shot 12, AD-6.

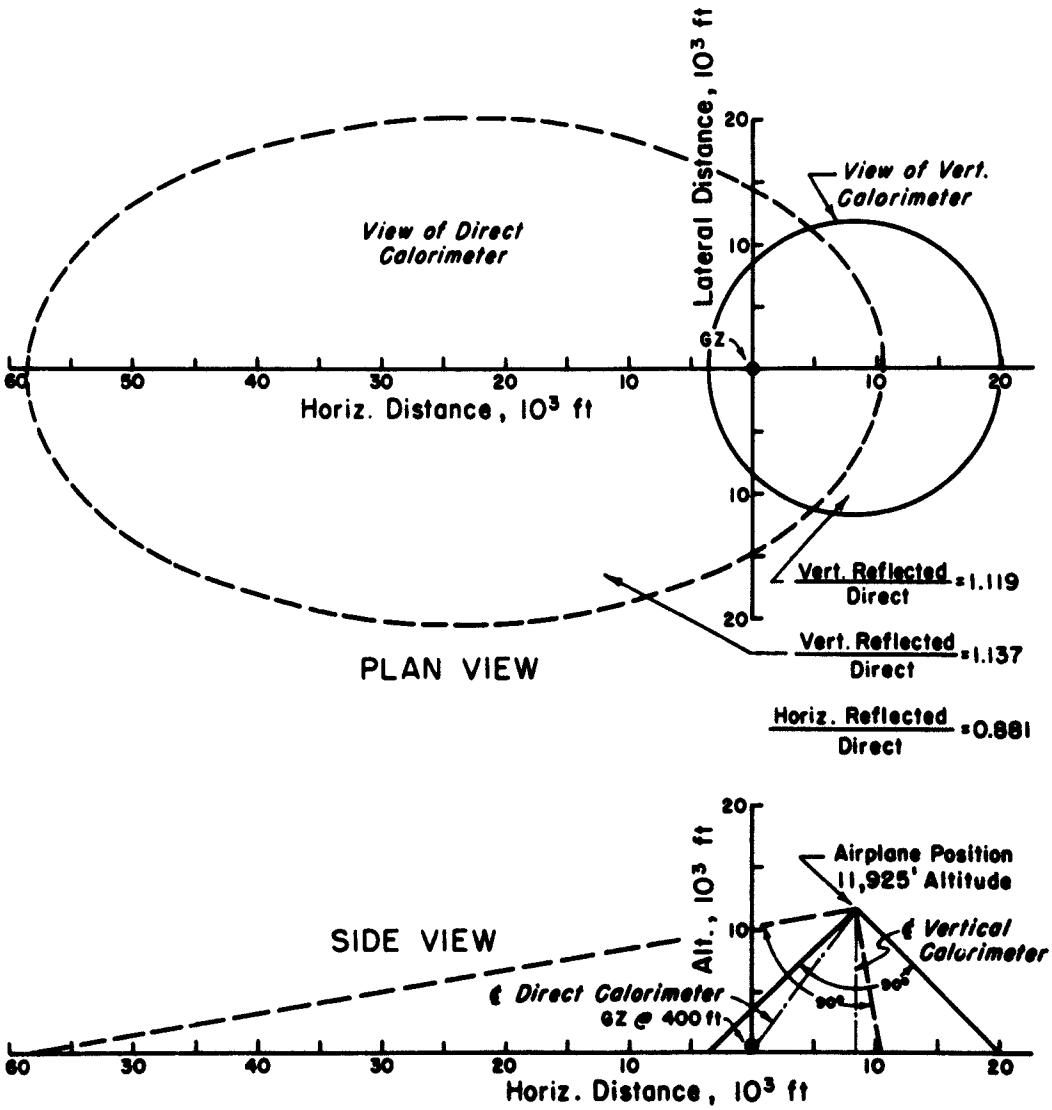

Figure 4.9 Airplane Position and Theoretical Ratios of Ground-Reflected to Direct Radiation, Shot 12, AD-5.

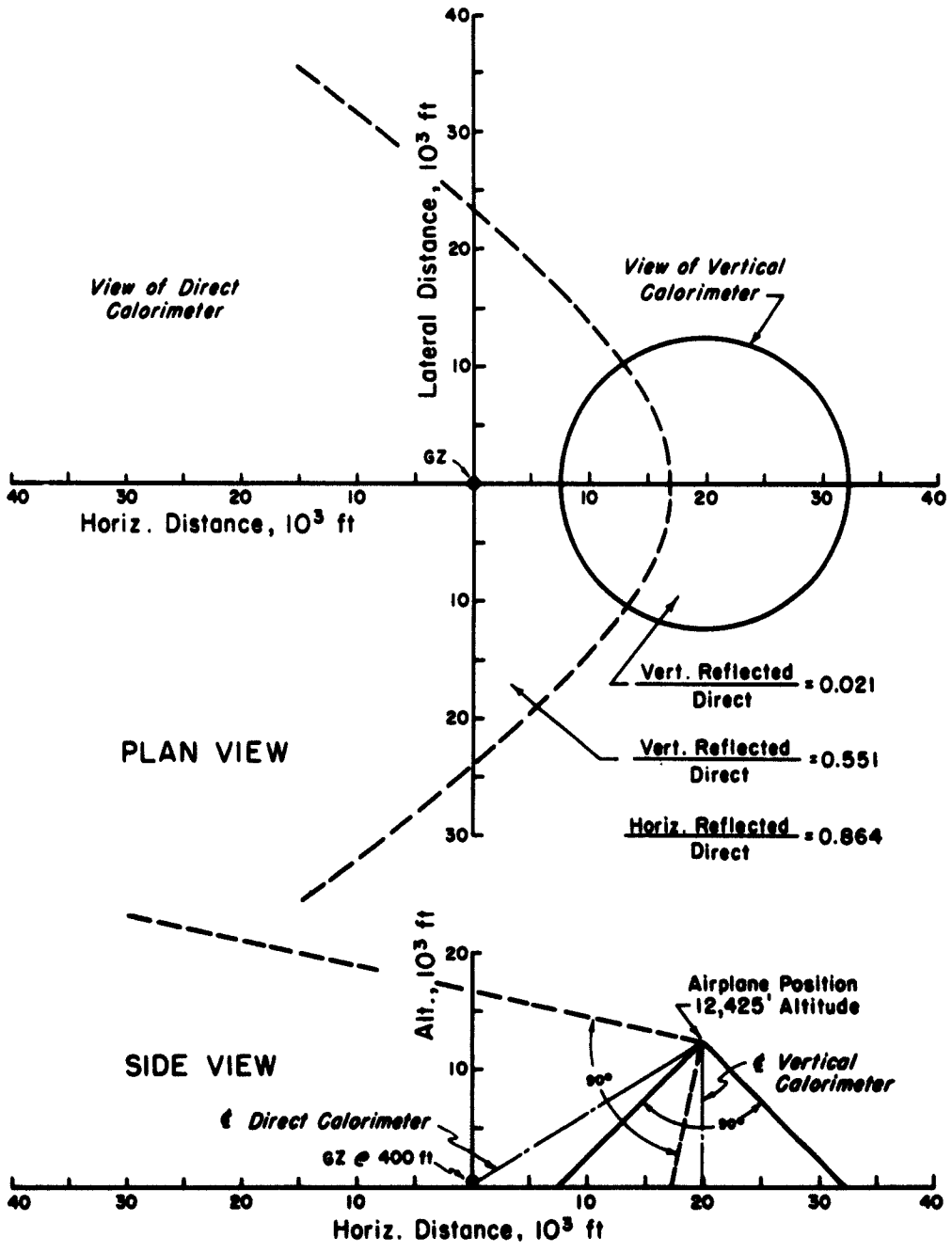

Figure 4.10 Airplane Position and Theoretical Ratios of Ground-Reflected to Direct Radiation, Shot 12, AD-4B.

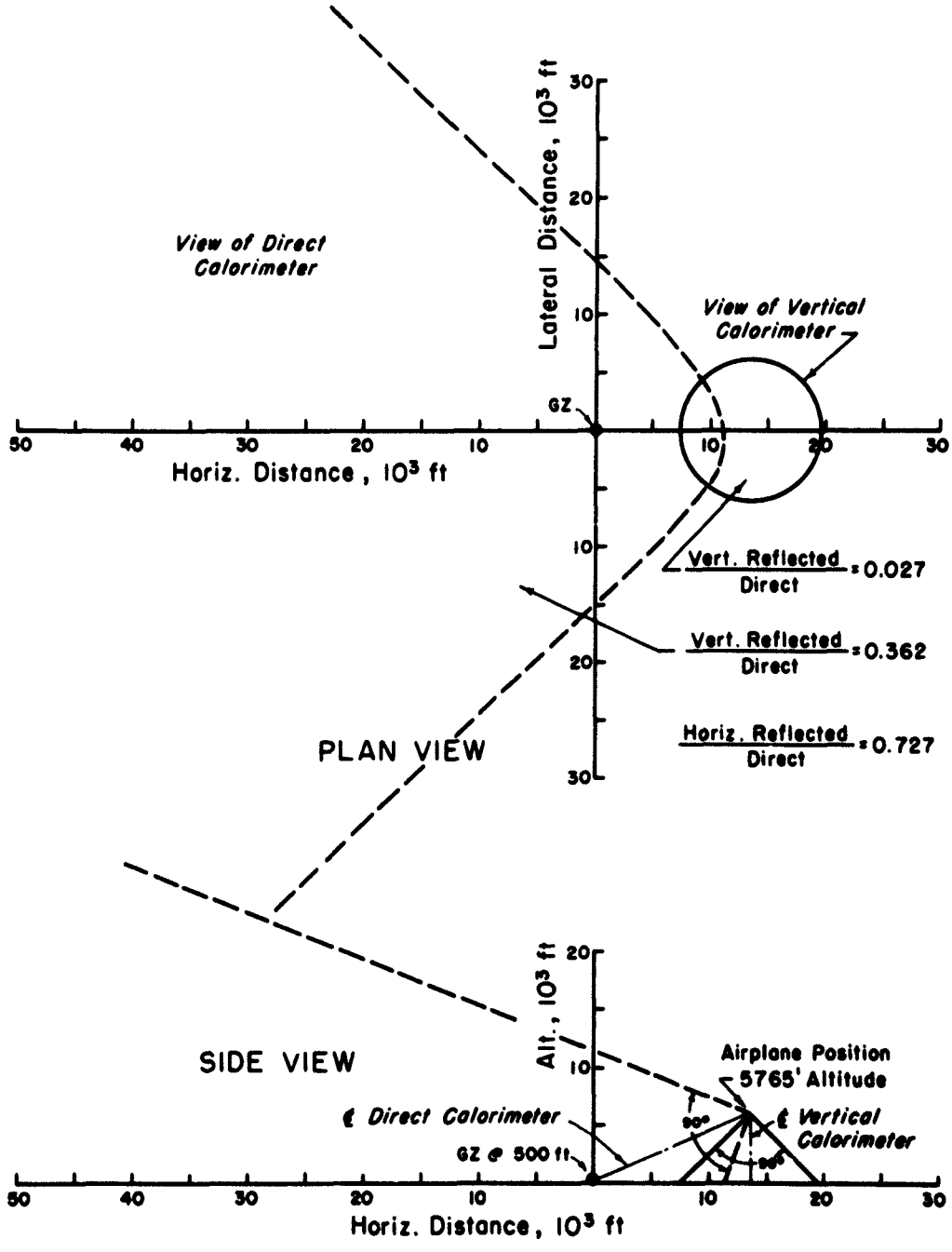

Figure 4.11 Airplane Position and Theoretical Ratios of Ground-Reflected to Direct Radiation. Shot 13, AD-4B.

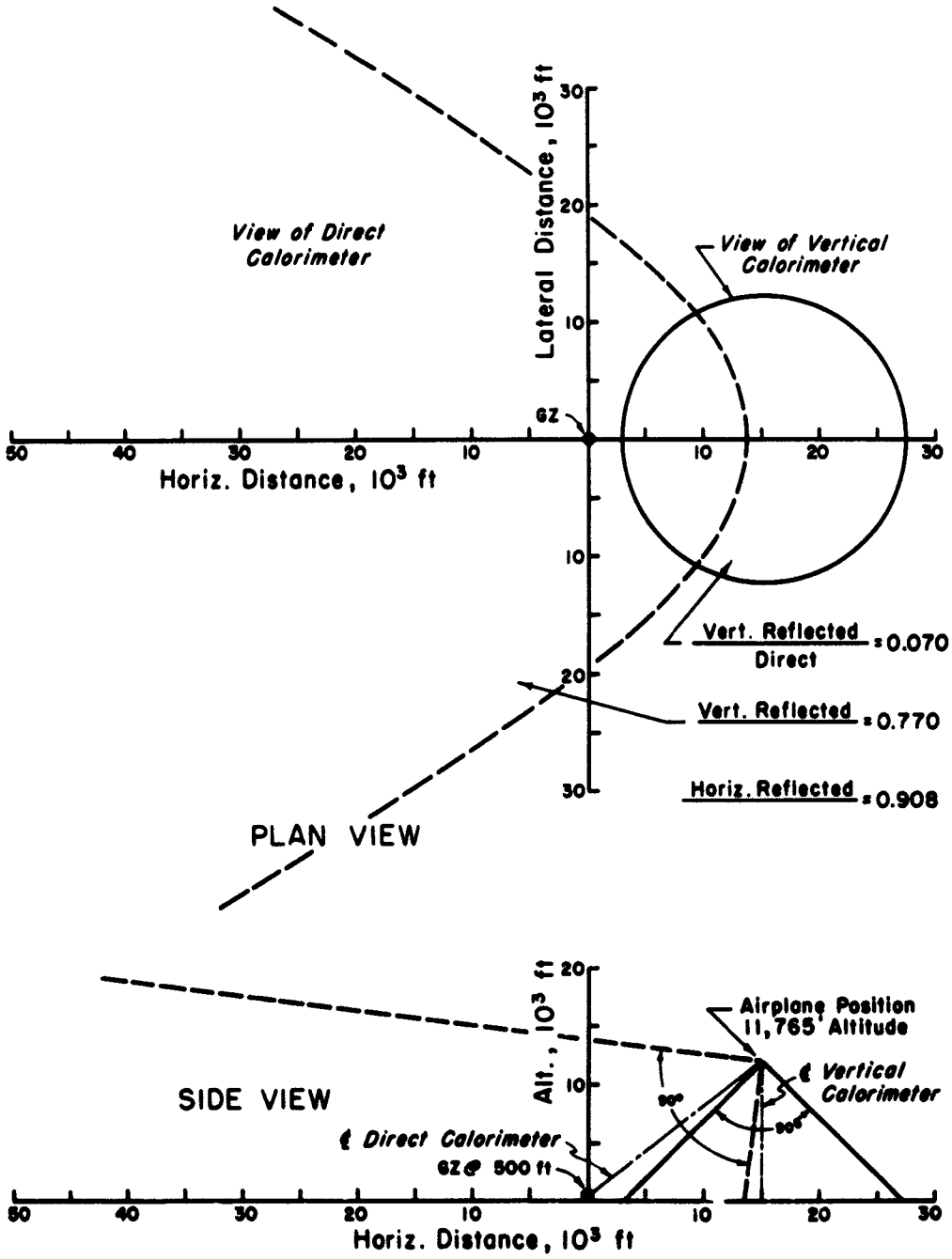

Figure 4.12 Airplane Position and Theoretical Ratios of Ground-Reflected to Direct Radiation, Shot 13, AD-5.

4.1.3 Correlation of Data. With the method outlined in 4.1.2 for direct radiation, the values of E_d* corrected for attenuation were determined and compared with the value of $W_{th}/4\pi R^2$ in Figure 4.13. In view of the good overall agreement and the small effect of scattered radiation, it is reasonable to conclude that the analytical approach to determine the contribution of reflected radiation yields values accurate to about ±10 percent. By the method outlined in 4.1.2 for indirect radiation, the calculated indirect energy, E_{ind}, expected at receivers was determined and compared with the measured indirect energy, E_{rm}, values in Figure 4.14. A summary of data used to derive Figures 4.13 and 4.14 is presented in the Appendix. If the above conclusion is correct concerning reflected radiation, then it follows that in the case where the reflected contribution is small, a good approximation for the scattered radiation is obtained. It should be noted that in Reference 9 a similar analysis of thermal data obtained during Operation CASTLE has given good correlation between predicted and measured values.

4.2 RECORDED THERMAL DATA

Figure 4.15 presents a comparison of recorded data with data of Reference 2. Except for Shot 12, Item Numbers 8 and 9, Table 3.1, where fireball distortion may have appeared, data agreement is fairly good. Some error in slant range distance may be

TABLE 4.1 PERCENT OF TOTAL DIRECT AND GROUND-REFLECTED FILTERED ENERGIES

Filter Type	Spectral Range of Transmission (Å)	Percent of Total Energy									
		Shot 4 AD-6 AD-4B		Shot 6 AD-5 AD-6		Shot 8 AD-5 AD-4B AD-6		Shot 12 AD-6 AD-5 AD-4B		Shot 13 AD-4B AD-5	
		Dir	Refl	Dir	Refl	Dir	Refl	Dir	Refl	Dir	Refl
Quartz	2,200 - 45,000	100	100	100	100	100	100	100	100	100	100
3-69	5,300 - 25,000	73	91*	84	100*	67	75	59	76	73	89*
		78	87	64	81	73	91*	67	74	67	100*
						69	75	72	70*		
2-58	6,400 - 25,000	62	91*	62	99*	51	38	47	65	59	85*
		59	63	—	87	63	74	57	38	63	78*
						—	70	—	61*		

*Horizontally distant test positions (15 percent atmospheric scattering).

present. MSQ controlled and formation aircraft are estimated to be within ± 300 feet and ± 800 feet horizontal distance from fireball, respectively. Figures 4.16 to 4.20 present normalized irradiance curves for all test conditions based on recorded radiometer time histories. Purely for information purposes, these curves from each shot are compared with a normalized field pulse of Reference 1.

4.3 SPECTRAL ENERGY DISTRIBUTION

Spectral energy measurements for the twelve test positions reported herein showed considerable random scatter in reflected-energy data. This is apparent in Table 4.1, where measured ground-reflected and direct energies under full spectrum clear Corning quartz filters are assumed as 100 percent. Relative to the 100 percent transmissivity for clear quartz, the ground-reflected energies for the same intensities under broad band 3-69 and 2-58 Corning filters were 100 to 70 percent and 90 to 38 percent, respectively. Similarly, direct energies were 84 to 64 percent and 63 to 47 percent, respec-

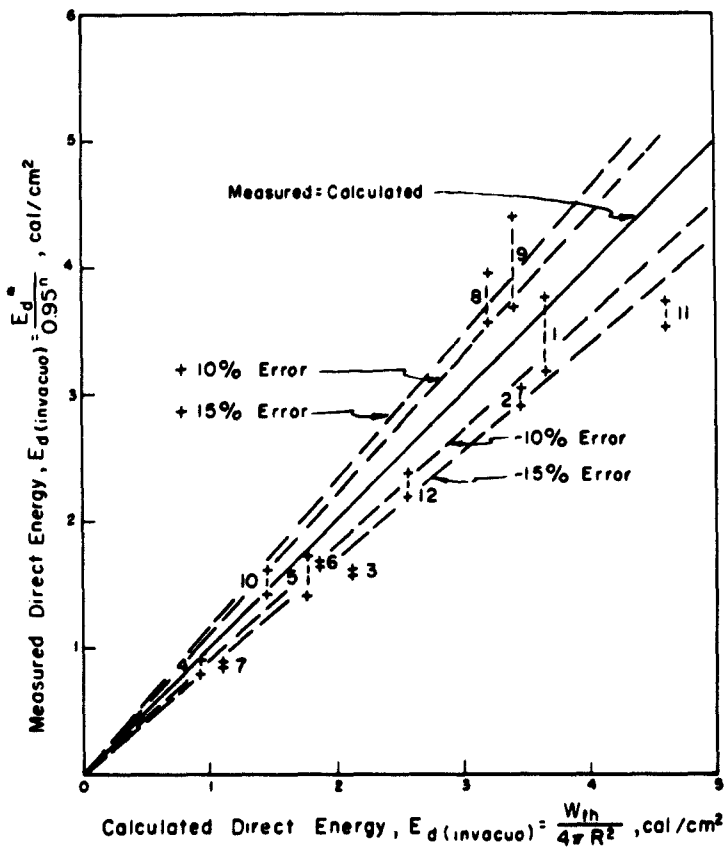

Figure 4.13 Measured versus Calculated Direct Energy Data.

tively. The indicated large random scatter in reflected-energy values prevent the establishment of a ground-reflected to direct energy spectral distribution ratio. Previously discussed phenomena related to atmospheric scattering and the effects of 90-degree-field-of-view calorimeter recordings of ground-reflected energies from finite areas at various test stations may suggest a contributing factor to this random scatter.

4.4 TEMPERATURE DATA

Figures 4.21 and 4.22 present plots of peak bare, white, and blue skin sample temperatures from Table 3.1. Approximately the same linear variation for shielded and unshielded temperature data in Figure 4.21 and 4.22, respectively, exist when plotted versus radiant energies. Surface finishes were undamaged up to maximum temperatures recorded. Checking these data against Figure 4.23 shows approximate absorbitivity coefficients for bare, white, and blue painted aluminum skin samples as 0.19, 0.14, and 0.45, respectively. This corresponds to 0.40, 0.20, and 0.60 in Reference 6. In a check on temperature rise times slant range versus total yield (Figures 4.24 and 4.25), a linear relationship also exists for bare, white, and blue painted aluminum skin samples, shielded and unshielded. As in Figure 4.15, and perhaps due to fireball distortion, Shot 12 points do not coincide with faired curves.

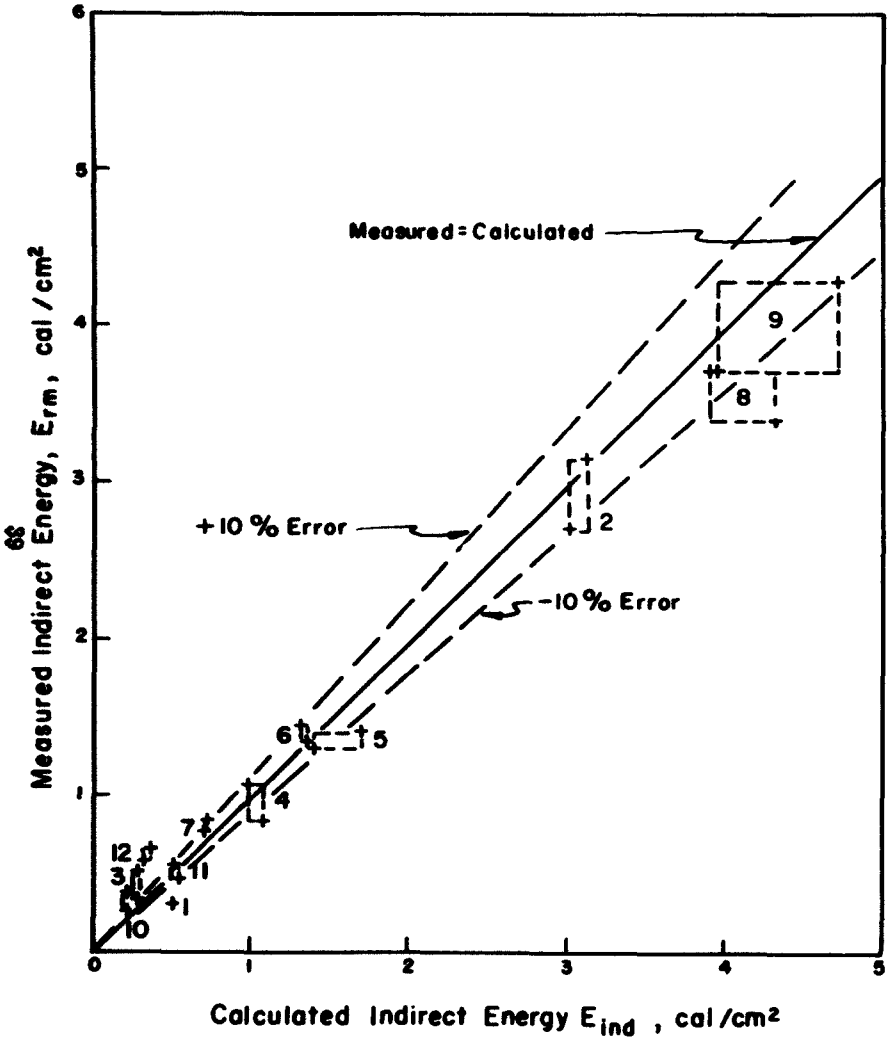

Figure 4.14 Measured versus Calculated Indirect Energy Data.

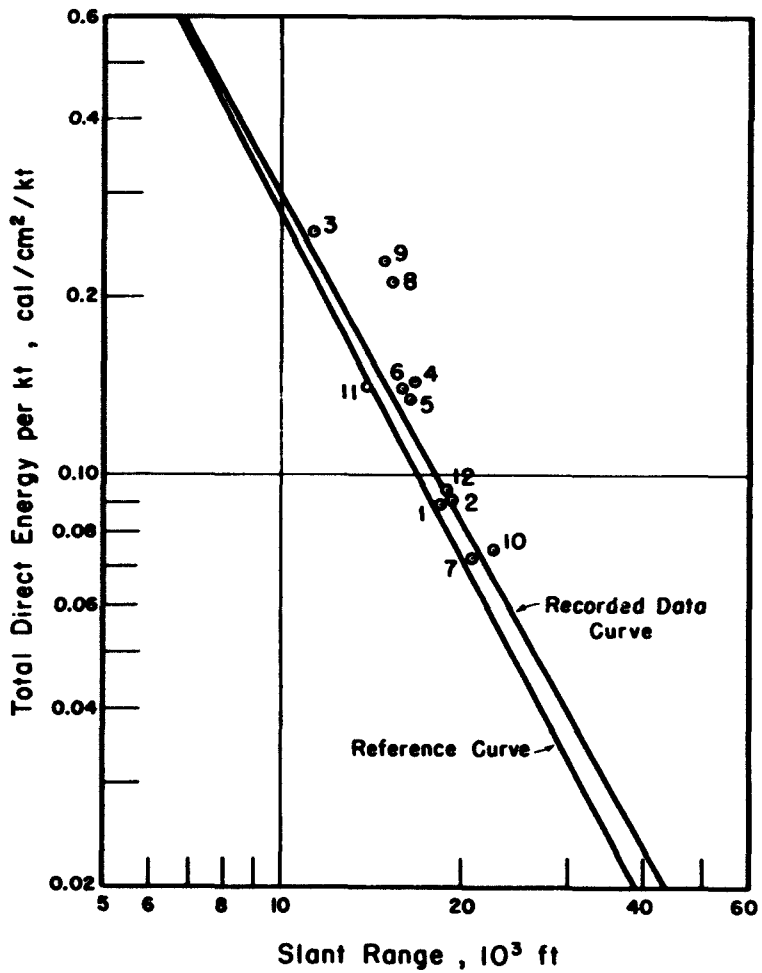

Figure 4.15 Energy per Kiloton versus Slant Range.

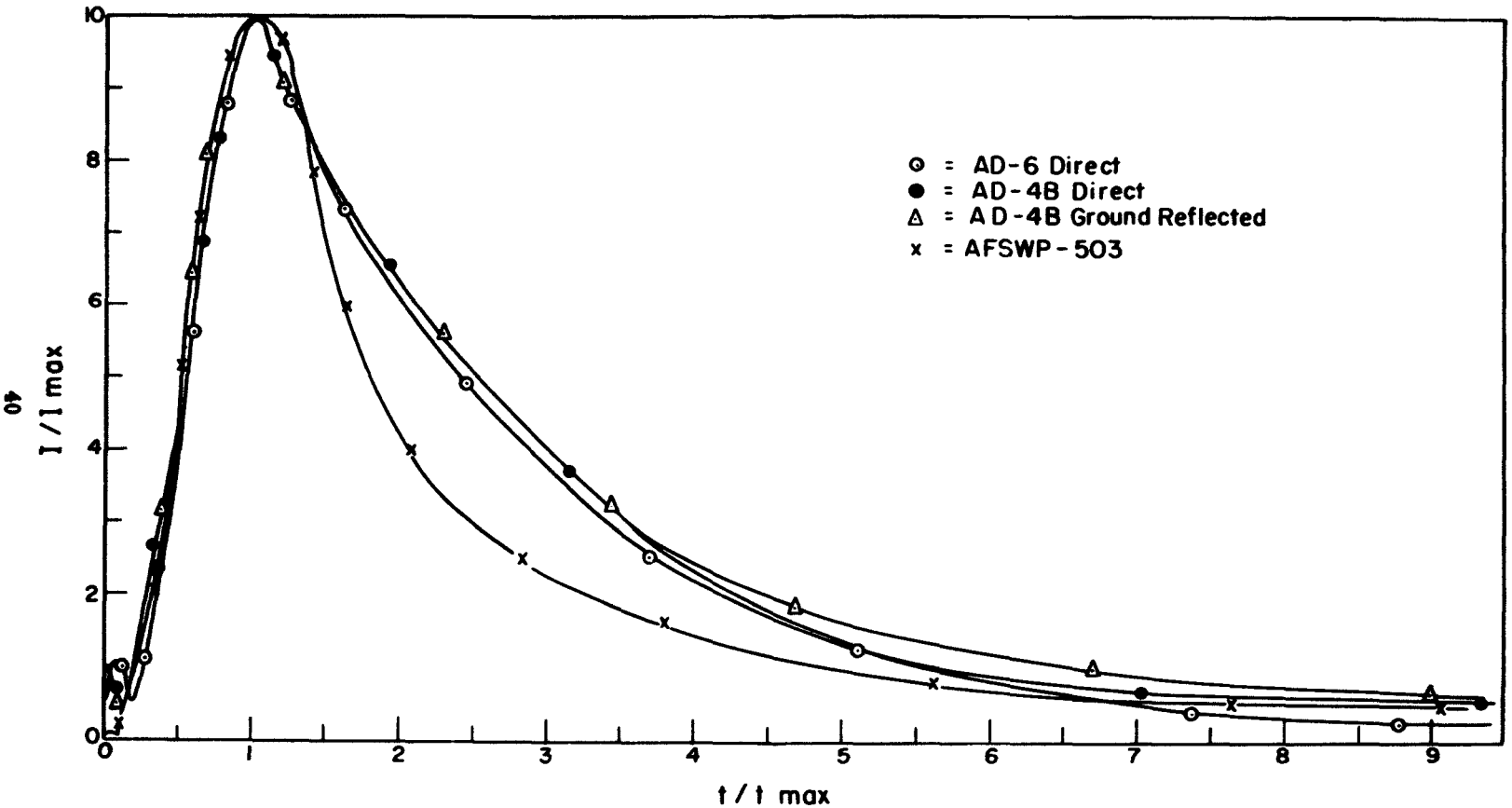

Figure 4.16 Normalized Irradiance and Generalized Field Pulse versus Time, Shot 4.

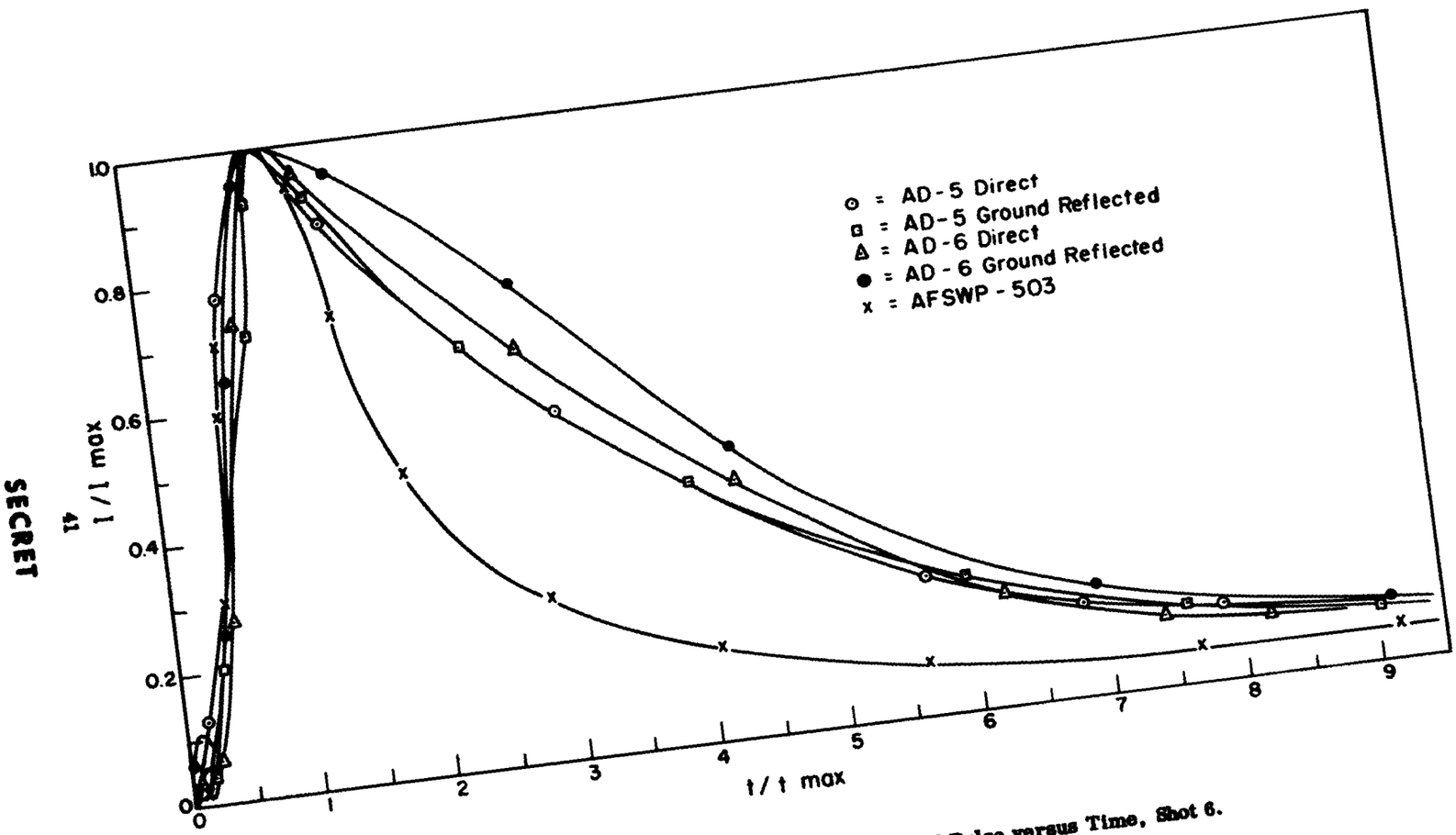

Figure 4.17 Normalized Irradiance and Generalized Field Pulse versus Time, Shot 6.

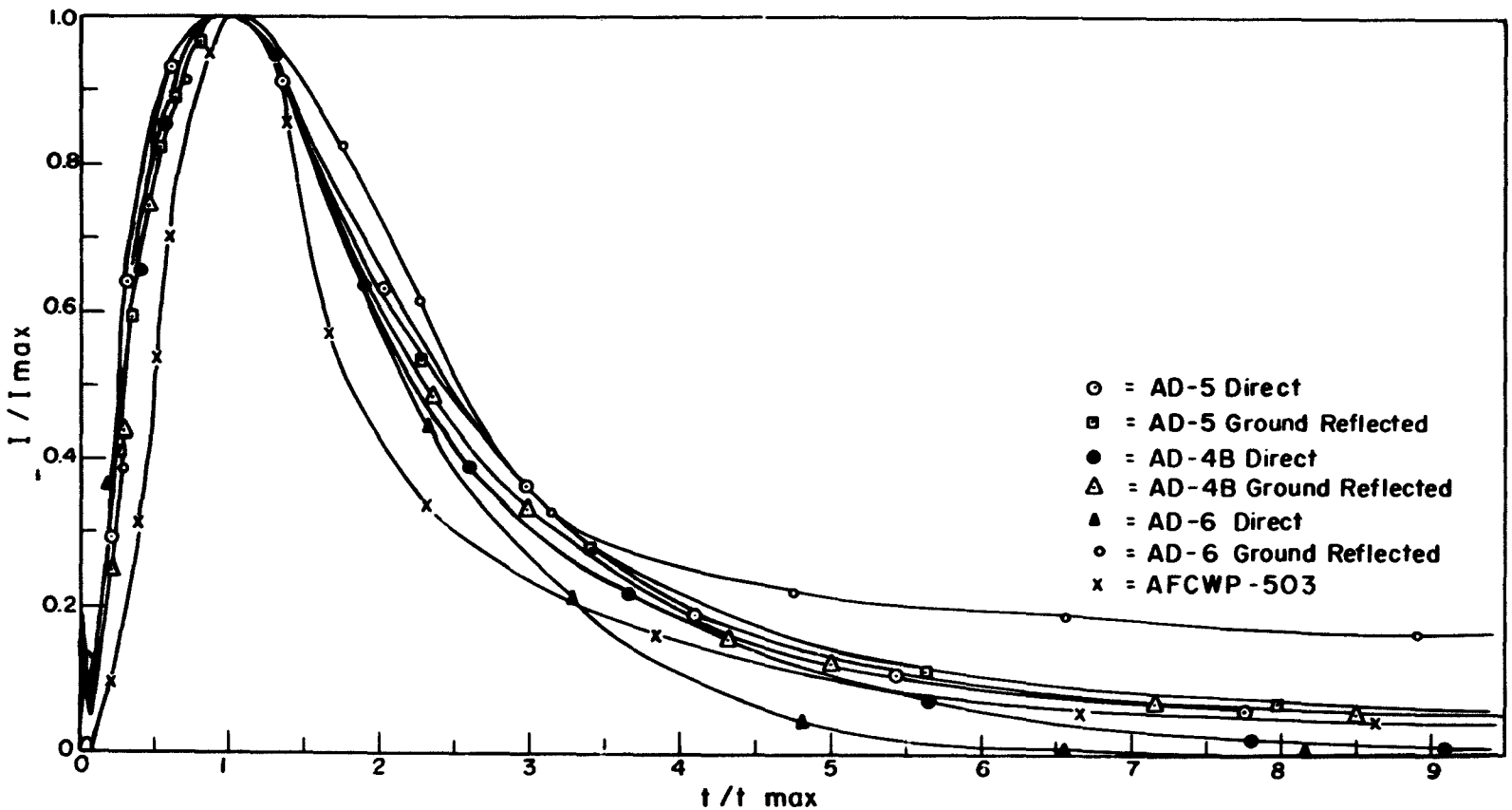

Figure 4.18 Normalized Irradiance and Generalized Field Pulse versus Time, Shot 8.

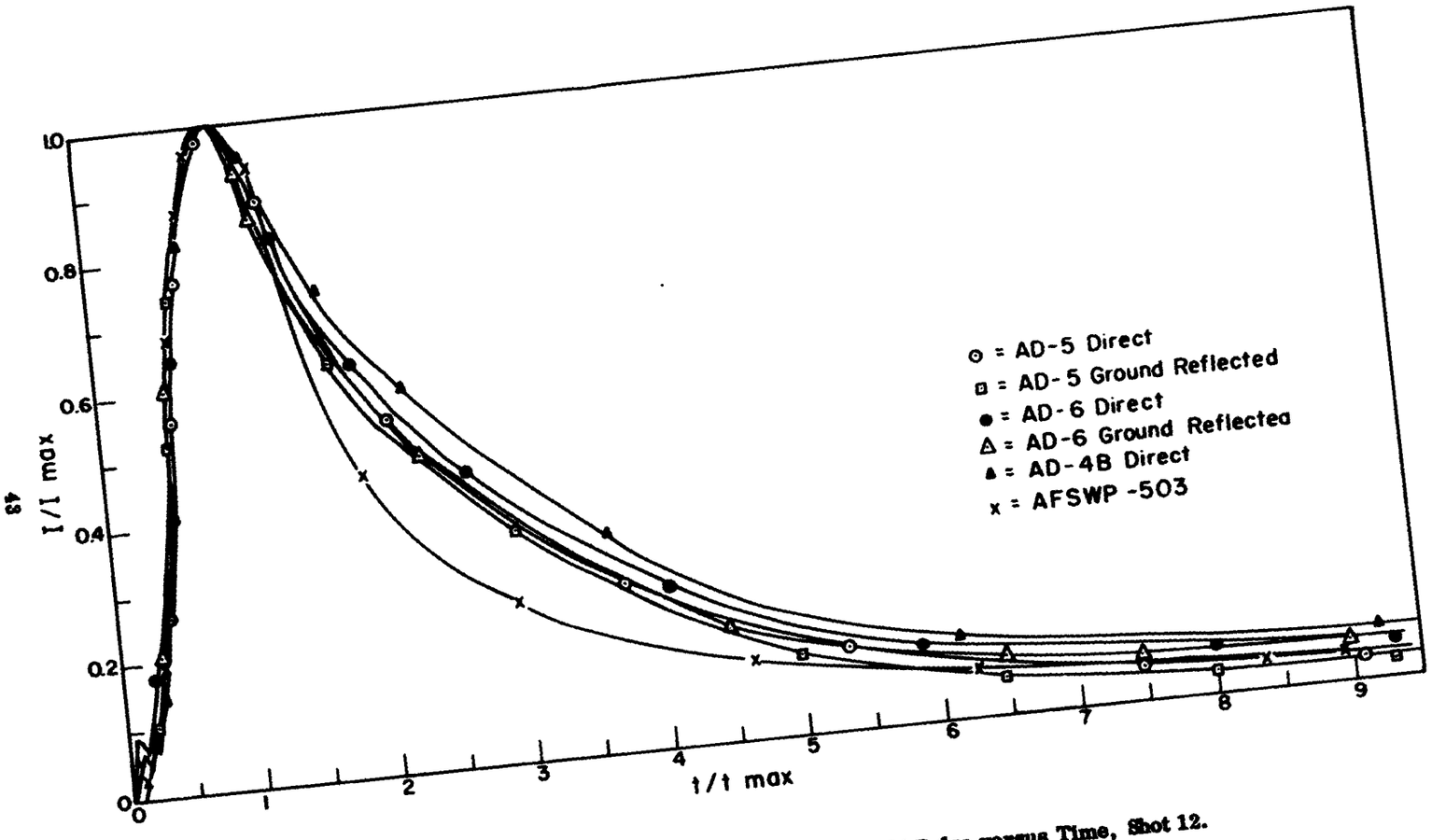

Figure 4.19 Normalized Irradiance and Generalized Field Pulse versus Time, Shot 12.

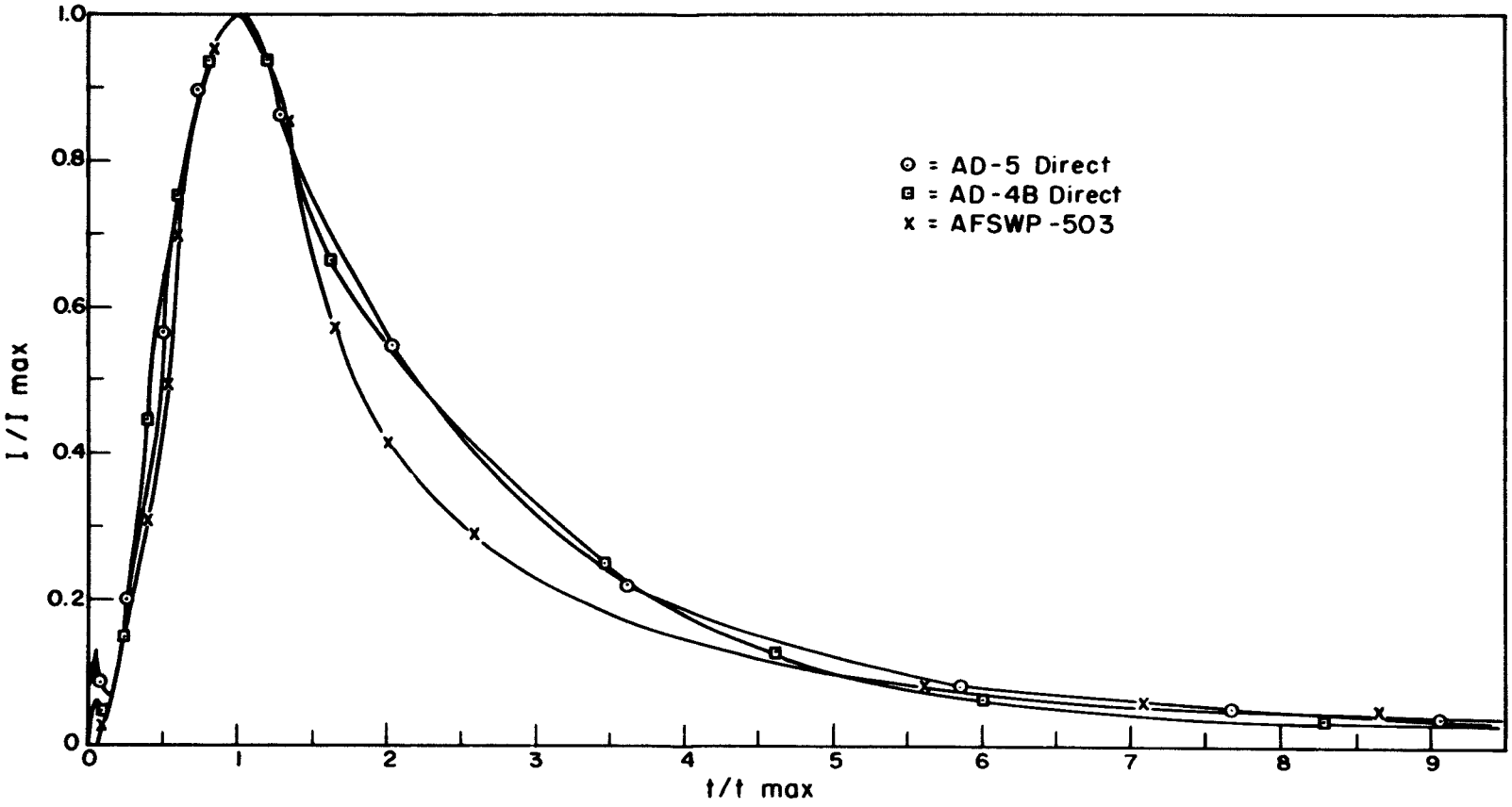

Figure 4.20 Normalized Irradiance and Generalized Field Pulse versus Time, Shot 13.

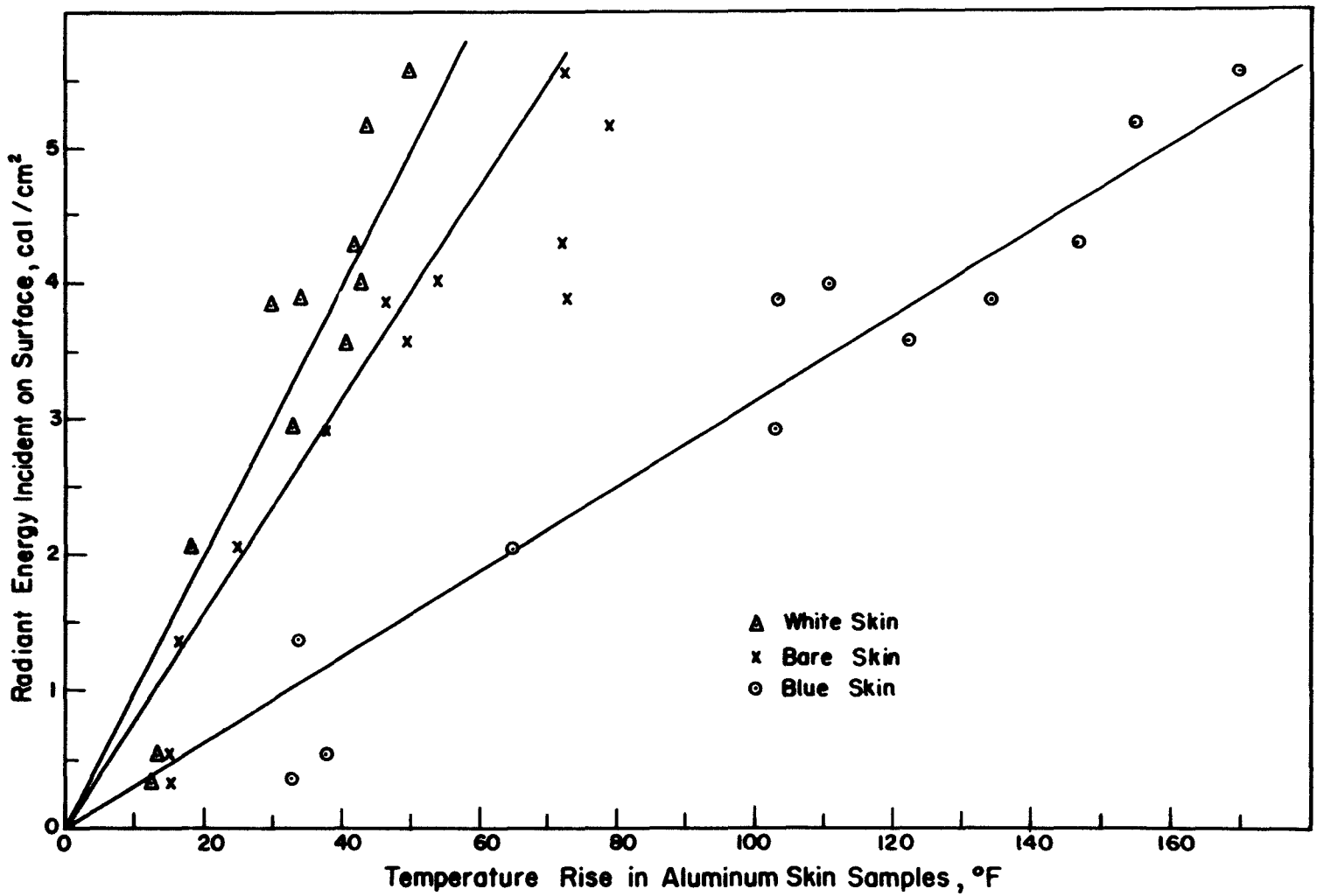

Figure 4.21 Energy versus Skin Temperature Curves. Note: Direct and ground-reflected energy through quartz filters.

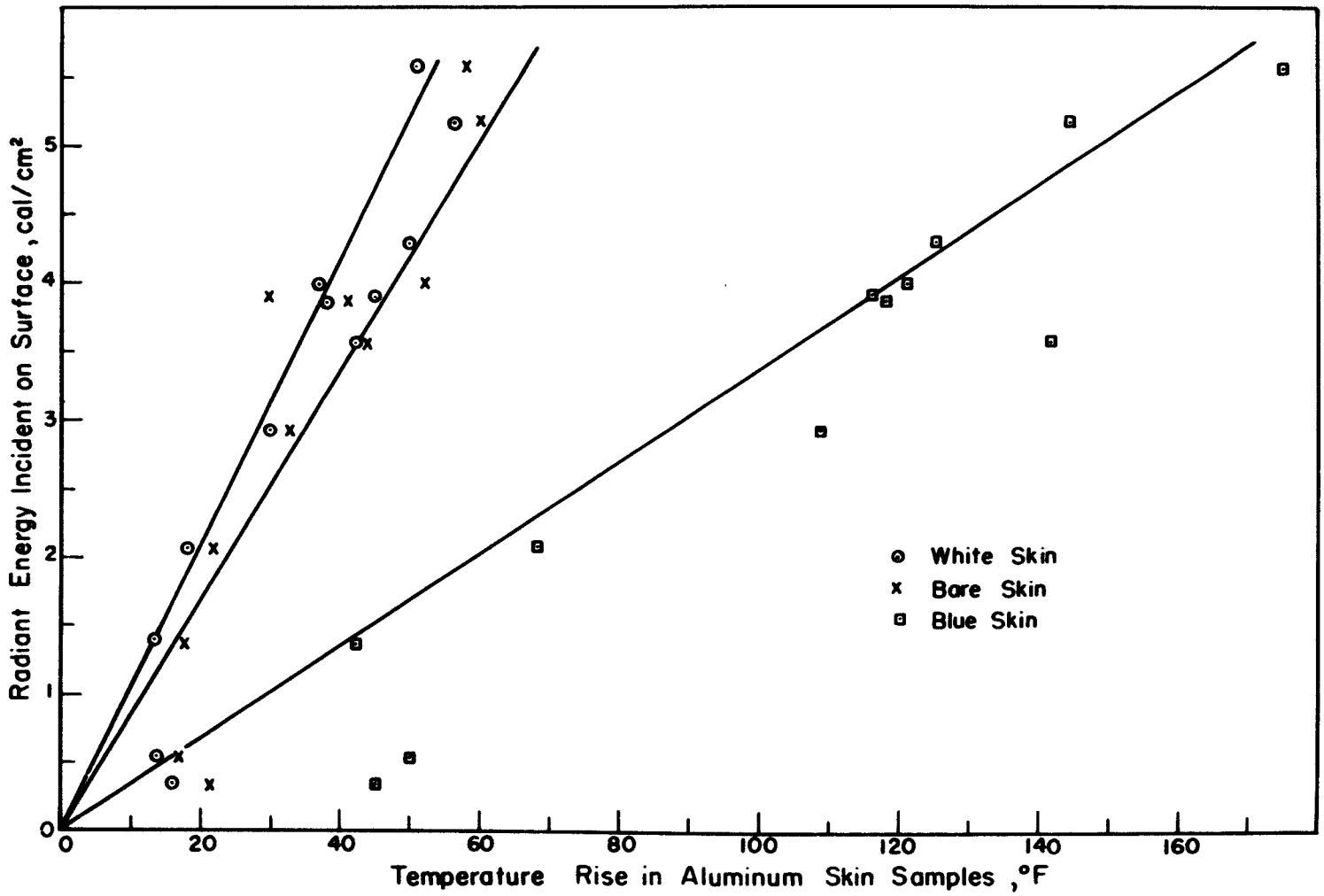

Figure 4.22 Energy versus Skin Temperature Curves. Note: Direct and ground-reflected energy through no filters.

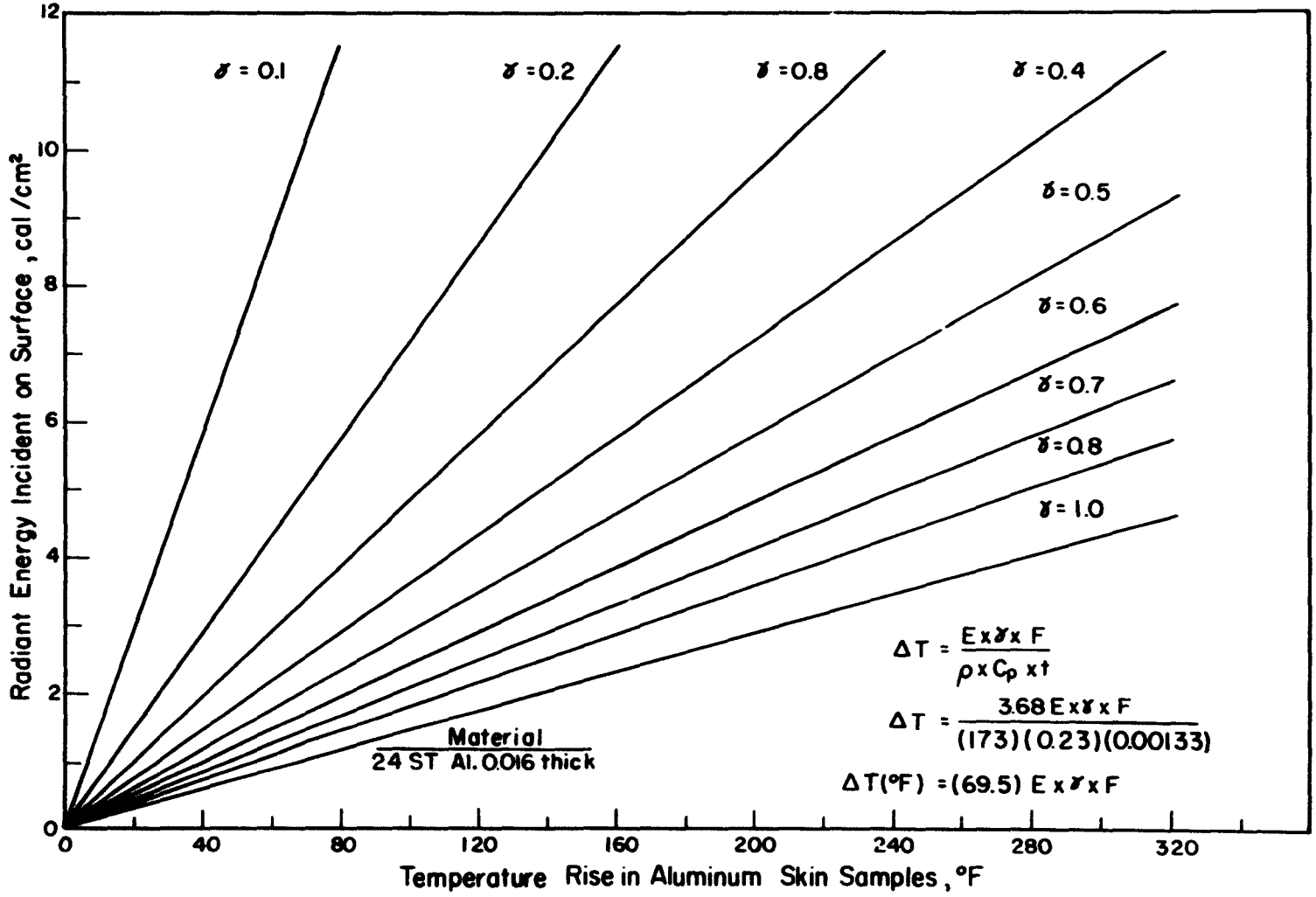

Figure 4.23 Temperature Rise versus Energy Curves.

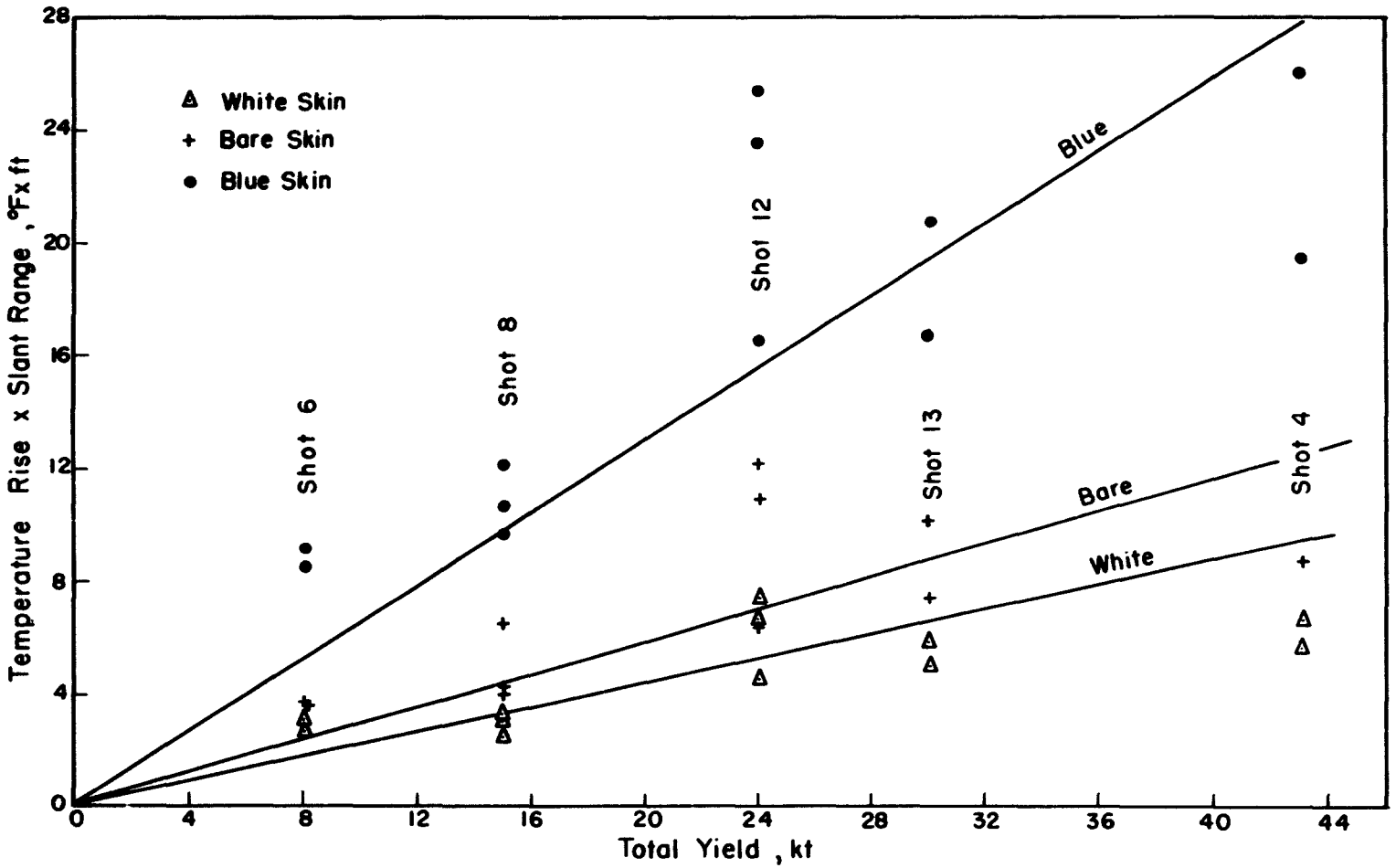

Figure 4.24 Temperature Rise times Slant Range versus Total Yield Curves. Note: Direct energy quartz filter.

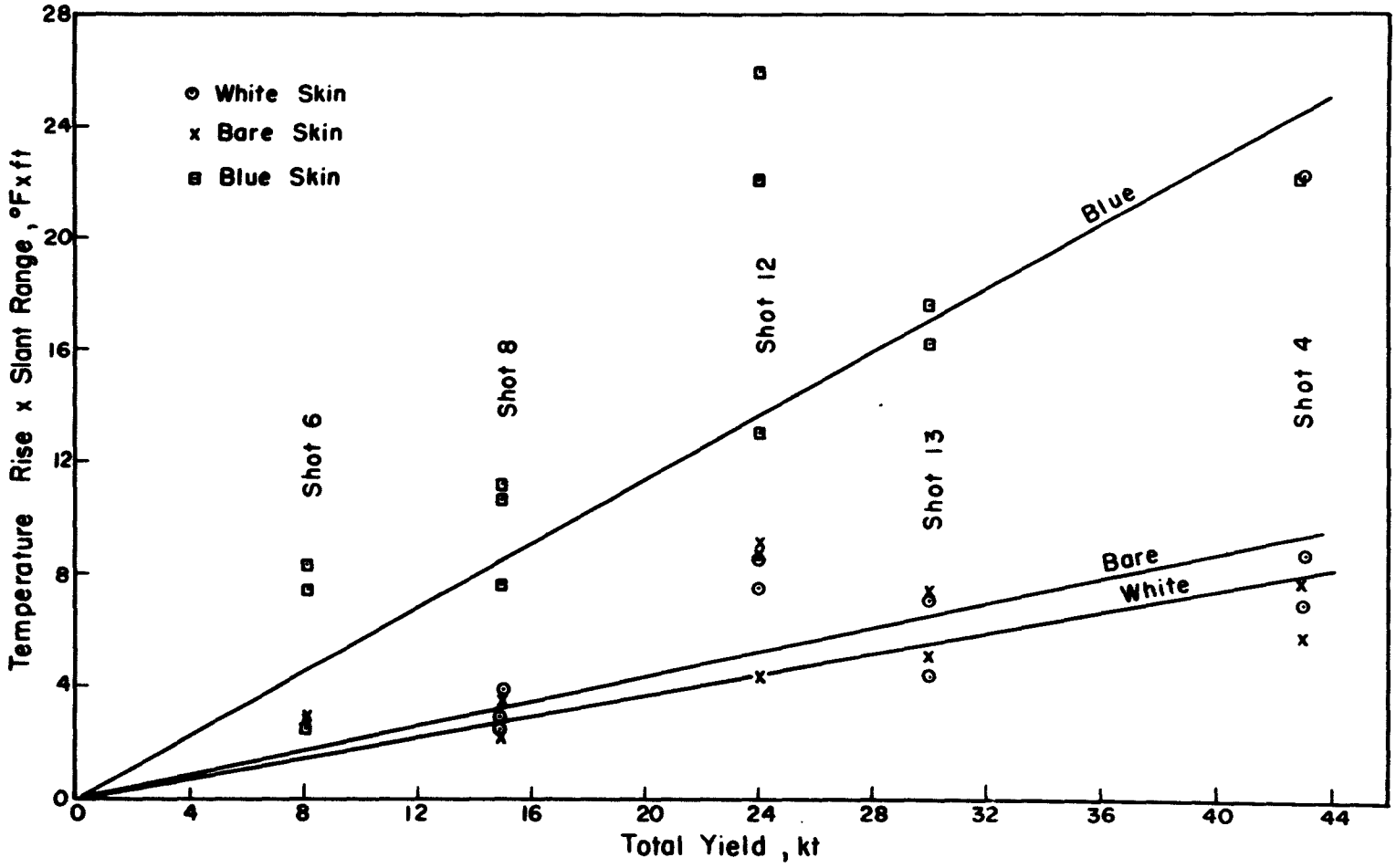

Figure 4.25 Temperature Rise times Slant Range versus Total Yield Curves. Note: Direct energy, no filter.

Chapter 5

CONCLUSIONS AND RECOMMENDATIONS

5.1 CONCLUSIONS

5.1.1 Experimental Check on Analytical Data. The theoretical values for the reflected radiation are, within 10 percent, comparable to the experimental values.

The contribution of atmospheric scattered radiation cannot be neglected and, in the case where fine particulate matter (like dust) exists in the vicinity of the explosion, the contribution of the scattered radiation increases.

5.1.2 Spectral Energy Distribution. Random scatter in ground-reflected energy measurements under broad-band filters (perhaps due to variation in the finite areas subtended by 90-degree-field-of-view indirect calorimeters at various test stations and related atmospheric scattering) prevents the establishment of a ground-reflected to direct energy spectral distribution ratio.

5.1.3 Temperature Data. Absorptivity coefficients from recorded data and data of Reference 6 show fair agreement for bare, white, and blue painted aluminum skin samples. Skin samples, exposed to and shielded against the airstreams show insignificant reduction in skin temperatures due to aerodynamic cooling. A maximum temperature rise of 175 degrees Fahrenheit was recorded at approximately 175 knots IAS. No apparent surface coating damages were observed.

5.1.4 Operational Success. All recording equipment performed in a satisfactory manner. Operational procedures and utilization of a thermal hood for pilot's protection against thermal radiation proved very satisfactory.

5.2 RECOMMENDATIONS

5.2.1 Thermal Data. It is recommended that analytical data for predicting ground-reflected thermal energy contributions to direct radiation be considered valid as a basis for use in the establishment of thermal effects envelopes for nuclear weapons. This recommendation is based on the assumption that proper allowance is made for ground-reflected and direct atmospheric attenuated and scattered energies.

It is further recommended that an experimental check of analytical data be made for weapons exceeding 43-kiloton total yield to further evaluate ground and atmospheric reflection, attenuation, and scattering effects. Utilization of 180-degree-field-of-view calorimeters and radiometers should be considered in this connection.

5.2.2 Temperature Data. It is recommended that a laboratory study be made of the effects of surface coating damage on the temperature rise and decay in aircraft skin samples utilizing field pulse inputs presented in this report in lieu of current rectangular pulse inputs.

Appendix

TABLE A.1 SUMMARY OF DIRECT ENERGY DATA COMPUTATIONS

SHOT NO.	TABLE 3.1 ITEM NO.	E_{dm}	$\left[1 + \beta \frac{E_r}{E_d} \kappa + \frac{E_s}{E_d^\circ}\right]$	E_d°	$(0.95)^n$	E_d(in vacuo)	$\frac{W_{th}}{4\pi R^2}$
4	1	4.19	1 + 0.329 + 0.05 = 1.334	3.14	0.833	3.77	3.66
		3.54		2.65		3.18	
	2	3.97	1 + 0.527 + 0.05 = 1.577	2.52	0.829	3.04	3.46
		3.81		2.42		2.92	
6	3	2.13	1 + 0.423 + 0.05 = 1.473	1.45	0.897	1.62	2.10
		2.07		1.41		1.57	
	4	1.25	1 + 0.57 + 0.05 = 1.62	0.772	0.85	0.908	0.94
		1.12		0.691		0.813	
8	5	2.24	1 + 0.49 + 0.05 = 1.54	1.46	0.852	1.71	1.77
		1.85		1.20		1.41	
	6	2.06	1 + 0.47 + 0.05 = 1.52	1.36	0.836	1.63	1.85
		2.13		1.40		1.68	
	7	1.07	1 + 0.48 + 0.05 = 1.53	0.70	0.818	0.855	1.11
		1.10		0.72		0.88	
12	8	5.42	1 + 0.544 + 0.05 = 1.592	3.40	0.862	3.94	3.2
		4.90		3.08		3.57	
	9	6.01	1 + 0.535 + 0.05 = 1.585	3.80	0.866	4.39	3.40
		5.08		3.20		3.69	
	10	1.71	1 + 0.445 + 0.05 = 1.495	1.14	0.802	1.42	1.45
		1.91		1.28		1.60	
13	11	4.40	1 + 0.302 + 0.05 = 1.352	3.25	0.871	3.72	4.6
		4.16		3.08		3.54	
	12	2.94	1 + 0.433 + 0.05 = 1.483	1.97	0.832	2.37	2.56
		2.70		1.82		2.19	

TABLE A.2 SUMMARY OF GROUND-REFLECTED ENERGY DATA COMPUTATIONS

SHOT NO.	TABLE 3.1 ITEM NO.	E_d°	$\left[\cos i + \beta \frac{E_{sr}}{E_d} \kappa + \frac{E_s}{E_d^\circ}\right]$	E_{ind}	E_{rm}
4	1	3.14	0 + 0.0089 + 0.15 = 0.1589	0.5	0.33
		2.65		0.42	0.33
	2	2.52	0.776 + 0.410 + 0.05 = 1.236	3.12	3.15
		2.42		3.00	2.70
6	3	1.45	0 + 0.0348 + 0.15 = 0.1848	0.27	0.53
		1.41		0.26	0.34
	4	0.772	0.848 + 0.49 + 0.05 = 1.388	1.07	0.83
		0.691		0.96	1.08
8	5	1.46	0.710 + 0.388 + 0.05 = 1.148	1.68	1.41
		1.20		1.38	1.31
	6	1.30	0.694 + 0.21 + 0.05 = 0.954	1.30	1.44
		1.40		1.34	1.31
	7	0.70	0.730 + 0.222 + 0.05 = 1.002	0.70	0.76
		0.72		0.72	0.83
12	8	3.40	0.785 + 0.429 + 0.05 = 1.264	4.30	3.39
		3.08		3.90	3.72
	9	3.80	0.772 + 0.415 + 0.05 = 1.237	4.70	4.27
		3.20		3.96	3.70
	10	1.14	0 + 0.00751 + 0.15 = 0.1575	0.18	0.28
		1.28		0.20	0.39
13	11	3.25	0 + 0.0101 + 0.15 = 0.16	0.52	0.48
		3.08		0.49	0.57
	12	1.97	0 + 0.0255 + 0.15 = 0.1755	0.35	0.66
		1.82		0.32	0.59

REFERENCES

1. Basic Characteristics of Thermal Radiation from an Atomic Detonation; AFSWP-503, November 1953; SECRET-RESTRICTED DATA.

2. Thermal Radiation from a Nuclear Detonation; Operation TUMBLER-SNAPPER, Project 8.3, WT-543, March 1953; SECRET-RESTRICTED DATA.

3. Preliminary Report on the Attenuation of Thermal Radiation from an Atomic or Thermonuclear Weapon; Air Force Cambridge Research Center, TN-54-25, November 1954;

3. Chapman, R. M., and Seavey, M. H.; Preliminary Report on the Attenuation of Thermal Radiation from an Atomic or Thermonuclear Weapon; Air Force Cambridge Research Center, Cambridge, Massachusetts, TN-54-25, November 1954; SECRET-RESTRICTED DATA.

4. Coulbert, C. D., and O'Brien, P. F.; Atmospheric Transmission of Thermal Radiation from Nuclear Weapons to Aircraft; Wright Air Development Center, Dayton, Ohio, TR 53-212, September 1953; SECRET-RESTRICTED DATA.

5. Reflection of Radiation from an Infinite Plane; Navy Department, Bureau of Aeronautics, Research Division Report Number DR-1434 (Part I) Revised June 1955; UNCLASSIFIED.

6. Guide to the Effects of Atomic Weapons on Naval Aircraft; Navy Department, Bureau of Aeronautics, Report NAVAER 00-25-536, July 1954; SECRET-RESTRICTED DATA.

7. Atomic Weapon Effects on AD Type Aircraft in Flight; Armed Forces Special Weapons Project, Operation UPSHOT-KNOTHOLE, Project 5.1, Report WT-748, March-June 1953; UNCLASSIFIED.

8. Instrumentation for Thermal Radiation Survey; Naval Air Materiel Center, Philadelphia, Pennsylvania, Report Number NAMC ASL 1006, to be issued; CONFIDENTIAL.

9. Zirkind, R.; Analysis of Thermal Radiation Emitted by a Nuclear Detonation; NAVAER Report Number DR-1740, to be published; SECRET-RESTRICTED DATA.

DISTRIBUTION

Military Distribution Category 5-30

ARMY ACTIVITIES

1 Asst. Dep. Chief of Staff for Military Operations, D/A, Washington 25, D.C. ATTN: Asst. Executive (R&SW)
2 Chief of Research and Development, D/A, Washington 25, D.C. ATTN: Atomic Division
3 Chief of Ordnance, D/A, Washington 25, D.C. ATTN: ORDTX-AR
4 Chief Signal Officer, D/A, P&O Division, Washington 25, D.C. ATTN: SIGRD-8
5 The Surgeon General, D/A, Washington 25, D.C. ATTN: Chief, R&D Division
6- 7 Chief Chemical Officer, D/A, Washington 25, D.C.
8 The Quartermaster General, D/A, Washington 25, D.C. ATTN: Research and Development Div.
9- 12 Chief of Engineers, D/A, Washington 25, D.C. ATTN: ENGNB
13 Chief of Transportation, Military Planning and Intelligence Div., Washington 25, D.C.
14- 16 Commanding General, Hdqs., U.S. Continental Army Command, Ft. Monroe, Va.
17 President, Board #1, Headquarters, Continental Army Command, Ft. Sill, Okla.
18 President, Board #2, Headquarters, Continental Army Command, Ft. Knox, Ky.
19 President, Board #3, Headquarters, Continental Army Command, Ft. Benning, Ga.
20 President, Board #4, Headquarters, Continental Army Command, Ft. Bliss, Tex.
21 Commanding General, U.S. Army Caribbean, Ft. Amador, C.Z. ATTN: Cml. Off.
22- 23 Commander-in-Chief, Far East Command, APO 500, San Francisco, Calif. ATTN: ACofS, J-3
24- 25 Commanding General, U.S. Army Europe, APO 403, New York, N.Y. ATTN: OPOT Div., Combat Dev. Br.
26- 27 Commanding General, U.S. Army Pacific, APO 958, San Francisco, Calif. ATTN: Cml. Off.
28- 29 Commandant, Command and General Staff College, Ft. Leavenworth, Kan. ATTN: ALLLS(AS)
30 Commandant, The Artillery and Guided Missile School, Ft. Sill, Okla.
31 Secretary, The Antiaircraft Artillery and Guided Missile School, Ft. Bliss, Texas. ATTN: Maj. Gregg D. Breitegan, Dept. of Tactics and Combined Arms
32 Commanding General, Army Medical Service School, Brooke Army Medical Center, Ft. Sam Houston, Tex.
33 Director, Special Weapons Development Office, Headquarters, CONARC, Ft. Bliss, Tex. ATTN: Capt. T. E. Skinner
34 Commandant, Walter Reed Army Institute of Research, Walter Reed Army Medical Center, Washington 25, D.C.
35 Superintendent, U.S. Military Academy, West Point, N.Y. ATTN: Prof. of Ordnance
36 Commandant, Chemical Corps School, Chemical Corps Training Command, Ft. McClellan, Ala.
37- 38 Commanding General, Research and Engineering Command, Army Chemical Center, Md. ATTN: Deputy for RW and Non-Toxic Material
39- 40 Commanding General, Aberdeen Proving Grounds, Md. ATTN: for Director, Ballistics Research Laboratory
41 Commanding General, The Engineer Center, Ft. Belvoir, Va. ATTN: Asst. Commandant, Engineer School
42 Commanding Officer, Engineer Research and Development Laboratory, Ft. Belvoir, Va. ATTN: Chief, Technical Intelligence Branch
43 Commanding Officer, Picatinny Arsenal, Dover, N.J. ATTN: ORDBB-TK
44 Commanding Officer, Frankford Arsenal, Philadelphia 37, Pa. ATTN: Col. Tewes Kundel
45 Commanding Officer, Army Medical Research Laboratory, Ft. Knox, Ky.
46- 47 Commanding Officer, Chemical Corps Chemical and Radiological Laboratory, Army Chemical Center, Md. ATTN: Tech. Library
48 Commanding Officer, Transportation R&D Station, Ft. Eustis, Va.
49 Director, Technical Documents Center, Evans Signal Laboratory, Belmar, N.J.
50 Director, Waterways Experiment Station, PO Box 631, Vicksburg, Miss. ATTN: Library
51 Director, Armed Forces Institute of Pathology, Walter Reed Army Medical Center, 6825 16th Street, N.W., Washington 25, D.C.
52 Director, Operations Research Office, Johns Hopkins University, 7100 Connecticut Ave., Chevy Chase, Md. Washington 15, D.C.
53- 55 Commanding General, Quartermaster Research and Development Command, Quartermaster Research and Development Center, Natick, Mass. ATTN: CBR Liaison Officer

NAVY ACTIVITIES

56- 57 Chief of Naval Operations, D/N, Washington 25, D.C. ATTN: OP-36
58 Chief of Naval Operations, D/N, Washington 25, D.C. ATTN: OP-03EG
59 Director of Naval Intelligence, D/N, Washington 25, D.C. ATTN: OP-922V
60 Chief, Bureau of Medicine and Surgery, D/N, Washington 25, D.C. ATTN: Special Weapons Defense Div.
61 Chief, Bureau of Ordnance, D/N, Washington 25, D.C.
62- 63 Chief, Bureau of Ships, D/N, Washington 25, D.C. ATTN: Code 348
64 Chief, Bureau of Yards and Docks, D/N, Washington 25, D.C. ATTN: D-440
65 Chief, Bureau of Supplies and Accounts, D/N, Washington 25, D.C.
66- 67 Chief, Bureau of Aeronautics, D/N, Washington 25, D.C.
68 Chief of Naval Research, Department of the Navy Washington 25, D.C. ATTN: Code 811
69 Commander-in-Chief, U.S. Pacific Fleet, Fleet Post Office, San Francisco, Calif.
70 Commander-in-Chief, U.S. Atlantic Fleet, U.S. Naval Base, Norfolk 11, Va.
71- 74 Commandant, U.S. Marine Corps, Washington 25, D.C. ATTN: Code A03H
75 President, U.S. Naval War College, Newport, R.I.
76 Superintendent, U.S. Naval Postgraduate School, Monterey, Calif.
77 Commanding Officer, U.S. Naval Schools Command, U.S. Naval Station, Treasure Island, San Francisco, Calif.
78 Commanding Officer, U.S. Fleet Training Center, Naval Base, Norfolk 11, Va. ATTN: Special Weapons School
79- 80 Commanding Officer, U.S. Fleet Training Center, Naval Station, San Diego 36, Calif. ATTN: (SPWP School)
81 Commanding Officer, Air Development Squadron 5, VX-5, U.S. Naval Air Station, Moffett Field, Calif.
82 Commanding Officer, U.S. Naval Damage Control Training Center, Naval Base, Philadelphia 12, Pa. ATTN: ABC Defense Course
83 Commander, U.S. Naval Ordnance Laboratory, Silver Spring 19, Md. ATTN: R
84 Commander, U.S. Naval Ordnance Test Station, Inyokern, China Lake, Calif.

85 Commanding Officer, U.S. Naval Medical Research Inst., National Naval Medical Center, Bethesda 14, Md.
86 Director, U.S. Naval Research Laboratory, Washington 25, D.C. ATTN: Mrs. Katherine H. Case
87 Director, The Material Laboratory, New York Naval Shipyard, Brooklyn, N. Y.
88 Commanding Officer and Director, U.S. Navy Electronics Laboratory, San Diego 52, Calif.
89- 92 Commanding Officer, U.S. Naval Radiological Defense Laboratory, San Francisco 24, Calif. ATTN: Technical Information Division
93 Commander, U.S. Naval Air Development Center, Johnsville, Pa.
94 Commanding Officer, Clothing Supply Office, Code 1D-0, 3rd Avenue and 29th St., Brooklyn 32, N.Y.
95 CINCPAC, Fleet Post Office, San Francisco, Calif.

AIR FORCE ACTIVITIES

96 Asst. for Atomic Energy, Headquarters, USAF, Washington 25, D.C. ATTN: DCS/O
97 Director of Operations, Headquarters, USAF, Washington 25, D.C. ATTN: Operations Analysis
98 Director of Plans, Headquarters, USAF, Washington 25, D.C. ATTN: War Plans Div.
99 Director of Research and Development, DCS/D, Headquarters, USAF, Washington 25, D.C. ATTN: Combat Components Div.
100-101 Director of Intelligence, Headquarters, USAF, Washington 25, D.C. ATTN: AFOIN-IB2
102 The Surgeon General, Headquarters, USAF, Washington 25, D.C. ATTN: Bio. Def. Br., Pre. Med. Div.
103 Asst. Chief of Staff, Intelligence, Headquarters, U.S. Air Forces Europe, APO 633, New York, N.Y. ATTN: Directorate of Air Targets
104 Commander, 497th Reconnaissance Technical Squadron (Augmented), APO 633, New York, N.Y.
105 Commander, Far East Air Forces, APO 925, San Francisco, Calif. ATTN: Special Asst. for Damage Control
106 Commander-in-Chief, Strategic Air Command, Offutt Air Force Base, Omaha, Nebraska. ATTN: Special Weapons Branch, Inspector Div., Inspector General
107 Commander, Tactical Air Command, Langley AFB, Va. ATTN: Documents Security Branch
108 Commander, Air Defense Command, Ent AFB, Colo.
109-110 Research Directorate, Headquarters, Air Force Special Weapons Center, Kirtland Air Force Base, New Mexico. ATTN: Blast Effects Research
111 Commander, Air Research and Development Command, PO Box 1395, Baltimore, Md. ATTN: RDDN
112 Commander, Air Proving Ground Command, Eglin AFB, Fla. ATTN: Adj./Tech. Report Branch
113-114 Director, Air University Library, Maxwell AFB, Ala.
115-122 Commander, Flying Training Air Force, Waco, Tex. ATTN: Director of Observer Training
123 Commander, Crew Training Air Force, Randolph Field, Tex. ATTN: 2GTB, DCS/O
124-125 Commandant, Air Force School of Aviation Medicine, Randolph AFB, Tex.
126-131 Commander, Wright Air Development Center, Wright-Patterson AFB, Dayton, O. ATTN: WCOSI
132-133 Commander, Air Force Cambridge Research Center, LG Hanscom Field, Bedford, Mass. ATTN: CRQST-2
134-136 Commander, Air Force Special Weapons Center, Kirtland AFB, N. Mex. ATTN: Library
137-138 Commander, Lowry AFB, Denver, Colo. ATTN: Department of Special Weapons Training
139 Commander, 1009th Special Weapons Squadron, Headquarters, USAF, Washington 25, D.C.
140-141 The RAND Corporation, 1700 Main Street, Santa Monica, Calif. ATTN: Nuclear Energy Division
142 Commander, Second Air Force, Barksdale AFB, Louisiana. ATTN: Operations Analysis Office
143 Commander, Eighth Air Force, Westover AFB, Mass. ATTN: Operations Analysis Office
144 Commander, Fifteenth Air Force, March AFB, Calif. ATTN: Operations Analysis Office
145 Commander, Western Development Div. (ARDC), PO Box 262, Inglewood, Calif. ATTN: WDSIT, Mr. R. G. Weitz

OTHER DEPARTMENT OF DEFENSE ACTIVITIES

146 Asst. Secretary of Defense, Research and Development, D/D, Washington 25, D.C. ATTN: Tech. Library
147 U.S. Documents Officer, Office of the U.S. National Military Representative, SHAPE, APO 55, New York, N.Y.
148 Director, Weapons Systems Evaluation Group, OSD, Rm 2E1006, Pentagon, Washington 25, D.C.
149 Armed Services Explosives Safety Board, D/D, Building T-7, Gravelly Point, Washington 25, D.C.
150 Commandant, Armed Forces Staff College, Norfolk 11, Va. ATTN: Secretary
151-156 Commander, Field Command, Armed Forces Special Weapons Project, PO Box 5100, Albuquerque, N. Mex.
157-158 Commander, Field Command, Armed Forces Special Weapons Project, PO Box 5100, Albuquerque, N. Mex. ATTN: Technical Training Group
159-169 Chief, Armed Forces Special Weapons Project, Washington 25, D.C. ATTN: Documents Library Branch
170 Office of the Technical Director, Directorate of Effects Tests, Field Command, AFSWP, PO Box 577, Menlo Park, Calif. ATTN: Dr. E. B. Doll

ATOMIC ENERGY COMMISSION ACTIVITIES

171-173 U.S. Atomic Energy Commission, Classified Technical Library, 1901 Constitution Ave., Washington 25, D.C. ATTN: Mrs. J. M. O'Leary (For DMA)
174-175 Los Alamos Scientific Laboratory, Report Library, PO Box 1663, Los Alamos, N. Mex. ATTN: Helen Redman
176-180 Sandia Corporation, Classified Document Division, Sandia Base, Albuquerque, N. Mex. ATTN: H. J. Smyth, Jr.
181-183 University of California Radiation Laboratory, PO Box 808, Livermore, Calif. ATTN: Clovis G. Craig
184 Weapon Data Section, Technical Information Service Extension, Oak Ridge, Tenn.
185-210 Technical Information Service Extension, Oak Ridge, Tenn. (Surplus)